

McGILL UNIVERSITY
Faculty of Graduate Studies and Research

AD 696697

**ESTIMATING THE TOPOGRAPHIC VARIATIONS
OF SHORT-WAVE RADIATION INCOME:
THE EXAMPLE OF BARBADOS**

by

B. J. GARNIER and ATSUMU OHMURA

Technical Report No. 1
under
Contract N00014-68-C-0307
NR 389-152
Department of the Navy, Office of Naval Research,
Geography Branch, Washington, D.C.
October, 1969

This document has been approved for Public Release and Sale;
its distribution is unlimited.

FOREWORD

This is the first of a series of Technical Reports which will be issued in respect of Contract No. NOG014-68-C-0307, NR 389-152 for a study of the Energy Budget of Barbados. The basic research, of which the contents of this Report represents an application, was performed with the financial assistance of the National Research Council of Canada and the Canadian Department of Transport (Meteorological Branch). Without this support the fundamental investigation leading to the development of the method for evaluating the surface variations of global radiation which is mainly the work of Mr. Atsumu Ohmura would not have been performed.

The maps and diagrams in this report were drawn by Mlle Nicole Demers, and the typing was done by Miss Daniela Stern.

B. J. Garnier
Principal Investigator

LIST OF FIGURES

1.	Location Map, Barbados	page	2
2.	Calculation of Sky-Diffuse Radiation on a Slope		12
3.	Computed and Measured Values of Global Radiation, Mont St. Hilaire, Quebec (lat. 45°N), Aug.29-Sept.2, 1968		16
4.	Computed and Measured Values of Sky-Diffuse Radiation Mont St. Hilaire, Quebec (lat. 45°N), Aug.29-Sept.2, 1968		18
5.	The Flow Diagram for the Basic Computer Programme to Calculate Direct Radiation on a Slope		20
6.	Computer Programme to Calculate Direct Radiation on a Slope		22
7.	Seasonal Change of the Latitude of Declination of the Sun		24
8.	Regions of Barbados for Relief Sampling		26
9.	Sampling Points and Gradient Angles for the Radiation Mapping Grid of Barbados		26
10.	Computer Programme for Calculating Global Radiation over Barbados		31
11.	A Sample of Global Radiation Values, Barbados		34
12.	Computer Programming to Map Global Radiation, Barbados		35
13.	Sample of Computer-Produced Map of Global Radiation over part of Barbados		38
14.	Computer Programme for Calculating Hourly Global Radiation in Barbados		40
15.	The Elevation of the Sun at Different Times on June 21, Barbados		42
16.	Atmospheric Transmissivity, Solar Radiation, and Sun Angle, Barbados		44
17.	A Sample of Hourly Global Radiation Values, Barbados		45

LIST OF TABLES

One	Table of Direct Radiation on Slopes, Barbados	page	23
Two	Solar Declinations Selected for Computer Programming		24
Three	Mean Daily Radiation Totals for Selected Months, 1964		49
Four	Selected Mean Hourly Radiation Totals, 1964		56

I

INTRODUCTION

The tropics has been known as a region of great heat for many centuries. The Greek division of the earth into "klimata" portrayed a "torrid" zone between the Tropics of Cancer and Capricorn, and Hadley's eighteenth century (Hadley, 1735) explanation of the causes of the trade winds was based on the idea of the excess heat of low latitudes causing equatorial air to rise and produce an inflow of air from north and south. Among more recent workers, Simpson (Simpson, 1930) calculated the atmospheric heat budget and showed the region within approximately 30° latitude of the equator to be one of positive heat balance throughout the year.

Most of the solar radiation which is the source of all this energy, passes through the atmosphere to the surface of the earth. Terrestrial long-wave radiation causes some loss of surface energy and gain of heat to the atmosphere, but the greater part of the heat received by the tropical atmosphere, and passed on to higher latitudes, is contributed by the turbulent and convective processes associated with the fluxes of latent and sensible heat from the tropical seas and lands. The exchange of energy at the tropical air/surface interface is thus extremely important to the global atmospheric circulation. Moreover, these transfers are frequently small-scale phenomena, even though they ultimately contribute to atmospheric circulation on the largest scale (Kuettnner and Holland, 1969). Thus, the surface exchanges in the tropics need to be studied in detail and on a microscale if their contribution

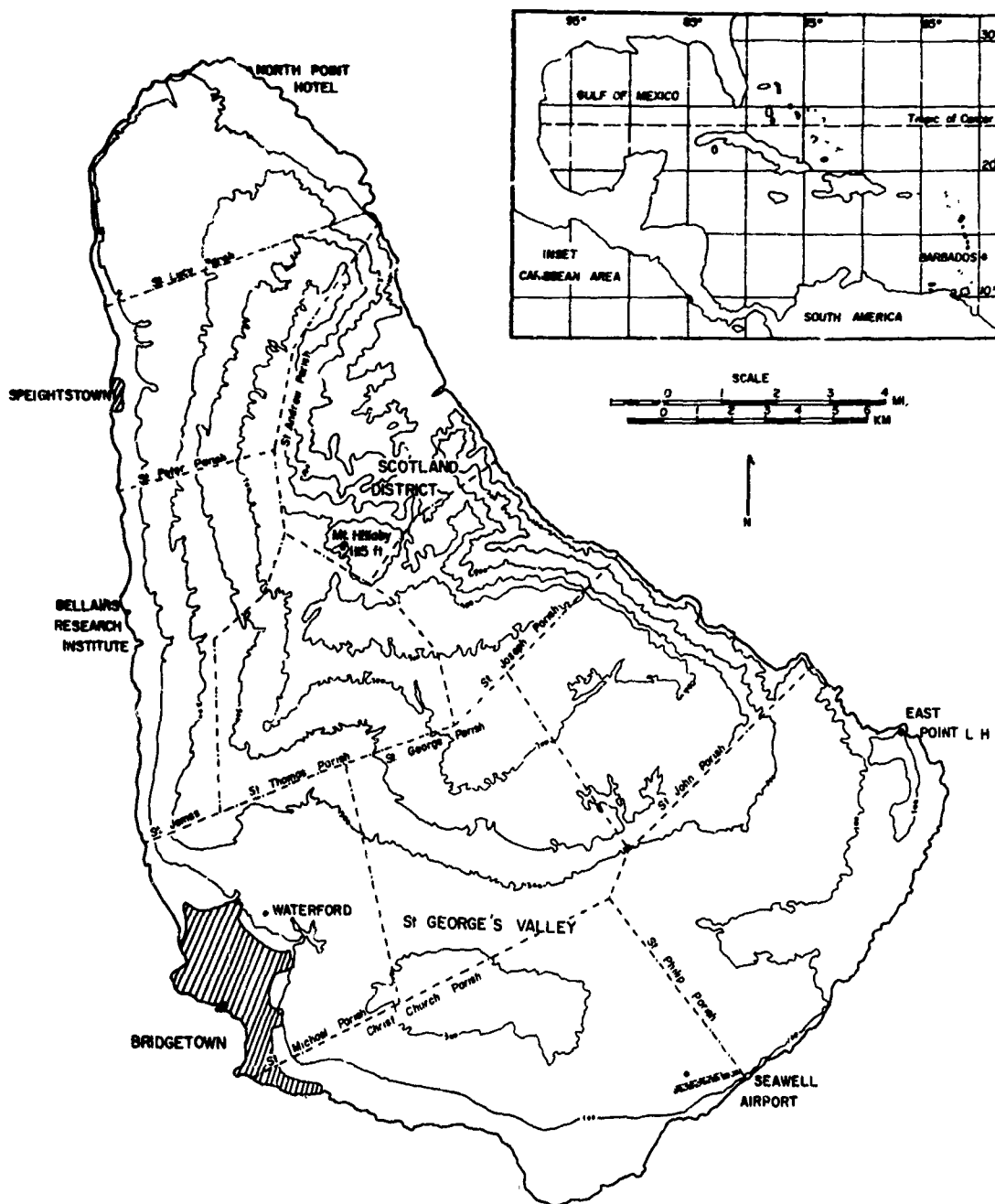


Fig. 1 Location Map: Barbados

to the atmospheric system is to be properly understood.

A great deal of attention is currently being paid to the air/sea interface within the tropics (Garstang and LaSeur, 1968; Kuettner and Holland, 1969). This is not surprising in view of the large amount of water lying within 30° latitude of the equator, the upper layers of which constitute a vast storehouse for the short-wave solar radiation received at the surface (Kuettner and Holland, 1969). The land areas of the tropics cannot, however, be neglected. Continental territories such as tropical Africa, tropical South America, and northern Australia, provide large areas of distinctive land-surface energy budgets, while scattered through the tropical oceans are numerous islands. The latter contribute to the atmospheric heat engine in two ways: by the energy balance of their surfaces; and by the turbulence arising from their nature as obstructions within prevailing, large-scale, oceanic wind-flow systems.

One such island is Barbados, the most easterly of the Leeward Islands of the West Indies, 13° latitude north of the equator, and located well within the trade wind belt of the North Atlantic ocean. There is no land between Barbados and the west coast of Africa. Thus, the island's 166 square miles of varied surface constitute a first obstruction in the moist, North Atlantic trade-wind flow after many miles of trans-oceanic passage. Such a location, in itself, provides a valuable base from which to study the influence of a heated island within the trade wind system (Garstang and LaSeur, 1968). The island is, however, both large enough and varied enough in surface character to provide a valuable base for sampling the energy budget of an island land surface under tropical conditions. In the south, where the island is widest, there is the

open, rolling country of the St. George Valley (Fig. 1). Immediately to the north the land rises rapidly and relief intensity increases. Mount Hiliaby, 1,115 feet above sea level and the island's highest point, is roughly the centre of a long north-south ridge which divides the island sharply across the line of the prevailing trade winds. The eastern side of the ridge is steep and deeply dissected; its western side slopes smoothly to the shores of the parishes of St. James and St. Peter, while gentle slopes also characterise the terrain descending towards Bridgetown. This relatively simple, yet strong, physiography thus offers sufficient variety to provide a base for studying how relief affects surface radiation and energy budget characteristics. At the same time, it does not produce so complicated a pattern as to develop a degree of diversity which defies analysis.

A manageable diversity within a relatively simple framework also characterises the surface expression of cultural activities. The cultivation of sugar cane dominates the agricultural scene. However, the legal requirement that ten per cent of plantation land should be in food crops, ensures the existence here and there of agricultural landscapes other than sugar cane growing, while the existence of Bridgetown, together with scattered areas of woodland and grassland, offers a total ensemble of cultural landscapes sufficient to enable the influence of these, as well as relief, to be incorporated into the energy budget investigations.

This combination of location, relief, and cultural influences thus makes Barbados a particularly suitable base for studying the surface energy balance of a tropical island. Such a study involves solving the

basic energy balance equations which for a land surface are:

$$R_N = (Q + q)(1 - a) + L\uparrow - L\downarrow \quad (1)$$

$$R_N - G = LE + H \quad (2)$$

where R_N is net radiation, Q is direct short-wave radiation, q is sky-diffuse short-wave radiation, $L\uparrow$ is long-wave emission from the atmosphere, $L\downarrow$ is long-wave emission from the ground, G is heat conduction in the ground surface, and LE and H are the latent and sensible heat fluxes respectively.

Both these equations have been evaluated by numerous scientists under a variety of conditions, both tropical and non-tropical. The instrumentation and techniques for their solution are, therefore, well known. As a rule the work has concentrated on observations at points for different kinds of horizontal surface. Such observations have provided an insight into the physical processes and diverse influences involved in the surface energy balance and earth/air interactions. For a realistic picture to emerge, however, it is necessary to evaluate also the surface variations in the balance of energy. This is particularly important in the tropics where solar energy is passed into the atmosphere from the surface, and where small-scale exchanges at the earth/air interface can have such important consequences for the circulation of the atmosphere at large.

It is common practice in climatology to evaluate the spatial distribution of phenomena from observations taken at points. Such an evaluation is as accurate as the basis on which the interpolation is made.

If this basis is weak, the resulting patterns of surface variation are poor, however, accurate the original point observations might have been. Thus it is important to understand the processes underlying a spatial distribution and to evaluate the surface variations in these terms from point observations, rather than to interpolate blindly from point observations which may only express the consequences of physical processes and which are not, therefore, in themselves a valid basis for drawing isarithmic lines of the element to be evaluated in spatial terms (Garnier, 1968).

It follows from this argument that to express the topographic variations of the radiation balance (equation (1)), or of the surface energy budget (equation (2)), it is necessary to see these as expressions of fundamental physical processes which can then be employed in spatial terms. Both equations express the interplay of three major factors: the influence of earth/sun relationships; the effect of the atmosphere, largely expressed through weather conditions; and the contribution of surface characteristics. These three factors can be classed respectively as macroscale, mesoscale, and microscale, in both a spatial and a temporal sense. Thus, earth/sun relationships are responsible for the fundamental earthward flux of energy which varies in a large-scale way with latitude and the season; atmospheric influences are largely mesoscale in character in terms of the synoptic scale of fundamental weather influences; and surface character operates at the microscale level by exercising final control over conditions at a given spot, within the framework provided by the other two elements.

Experimental work currently proceeding in Barbados can measure the parameters of both equations (1) and (2). These measurements become

spatially meaningful when they are applied in terms of the fundamental approach indicated above. This provides a rational way to solve the radiation balance and energy budget equations in terms of their topographic variations. Such an approach, moreover, does not necessarily require a close network of observation points (Garnier, 1968).

Although the ultimate aim is to try to solve both equations (1) and (2) in this way, the initial concentration has been on the solution of equation (1). This expresses R_n in terms of shortwave and longwave radiation balances. The work to date has emphasised the topographic variation of shortwave radiation income ($Q + q$) the evaluation of which from the observations of a single, representative site can now be satisfactorily achieved (Garnier and Ohmura, in press). This evaluation is fundamental to the solution of equation (1) and also involves the most intricate calculations. The purpose of this report is principally to discuss the methods used and to show some of the results achieved. Work on the evaluation of the other elements of equation (1) is currently proceeding and will be reported on in due course.

II

THE EVALUATION OF SURFACE VARIATIONS IN GLOBAL RADIATION INCOME

In order to evaluate the surface variations of global radiation income, it is necessary to calculate the direct and sky-diffuse components separately, and to sum the results. This is because the source of direct radiation is different from that of sky-diffuse: the former comes directly from the sun acting as a single source in terms of its position in the sky; sky-diffuse radiation, on the other hand, comes from diverse sources depending partly on the position of the sun in the sky and partly on the composition of the atmosphere, especially its cloudiness, at a given time. While the contribution from both sources can be treated theoretically and mathematically, the calculation of topographic variations of direct radiation is simpler than that of sky-diffuse radiation, and will be considered first.

Evaluation of Direct Solar Radiation Income

The integration over all wavelengths of the fundamental formula for the monochromatic intensity of the solar beam yields a general law of transmission (Haltiner and Martin, 1957) for the flux of direct solar radiation such that:

$$I_m = I_r p^m \quad (3)$$

where I_m is the energy in langley's per minute delivered by the sun on

a surface normal to the sun's rays, I_r is the value of extra-terrestrial radiation equal to the solar constant divided by the square of the radius vector of the earth, p is the mean-zenith-path transmissivity of the atmosphere, and m is the optical air mass.

The flux of direct solar energy falling on a surface is, however, only equal to I_m under the particular situation that the surface is, in fact, normal to the sun's rays. For all other cases, the intensity of radiation falling on a surface is the value of I_m modified by the relation between the angle and azimuth of the surface on the one hand, and the height and azimuth of the sun on the other. By expressing these characteristics of the surface and the sun by means of unit co-ordinate vectors, an equation can be derived to express the flux per minute of direct radiation on any surface in the form:

$$I_s = I_r p^m \cos(\underline{X} \wedge \underline{S}) \quad (4)$$

where I_s is the intensity of the shortwave radiation in langley's per minute falling on the surface, \underline{X} is a unit co-ordinate vector normal to the surface and pointing away from the ground, \underline{S} is a unit co-ordinate vector expressing the position of the sun, and \wedge is a symbol denoting the angle between \underline{X} and \underline{S} .

This equation can operate in several ways. The way chosen in the present context is to think of the sun as moving north and south with the seasons along the meridian of solar noon, and to consider the surface as rotating around the earth's polar axis once in twenty-four hours. This concept enables \underline{S} to be expressed solely in terms of the cosine and sine of the sun's angle of declination (δ), and \underline{X} to be expressed in terms of

the latitude of the surface (θ), its angle of slope (given by the zenith angle (Z_x) of \underline{X}), and the azimuth (A) of the surface. It can then be shown (Garnier and Ohmura, 1968; Ohmura 1969) that, for a given moment of time:

$$\begin{aligned} \cos(\underline{X} \wedge \underline{S}) = & 1(\sin\theta \cos H)(-\cos A \sin Z_x) - \sin H(\sin A \cos Z_x) \\ & + (\cos\theta \cos H) \cos Z_x \cos \delta + [\cos\theta (\cos A \sin Z_x) \\ & + \sin\theta \cos Z_x] \sin \delta \end{aligned} \quad (5)$$

where H is the hour angle measured from solar noon positively towards west and A is measured positively from north through east and negatively from north through west.

Equation (5) indicates that the value of $\cos(\underline{X} \wedge \underline{S})$ can be derived without difficulty from surface geometry and other readily available data. The value of m in equation (4) can also be derived in terms of the components used to express \underline{X} and \underline{S} provided that the secant approximation for the value of m can be used. Under these conditions (Garnier and Ohmura, 1968);

$$m = 1/\cos Z_s = 1/(\cos \delta \cos \theta \cos H + \sin \delta \sin \theta) \quad (6)$$

where Z_s is the zenith angle of the sun. When Z_s exceeds 70° , however, the secant approximation for m is invalid and the true value of the optical air mass as given, for example, in the Smithsonian Meteorological Tables (List, 1966, p. 417) must be used.

The only element of equation (4) which cannot be obtained from tables, earth/sun relationships, or terrain analysis, is atmospheric transmissivity (p). This is a highly variable quantity, being in a general way a function of the weather and prevailing air mass characteristics. The calculation of p for cloudless conditions can be made by standard methods (de Brichambaut, 1963). However, the procedure for evaluating direct radiation suggested here assumes the existence of observations at a site representative of the region over which the surface variations in short-wave radiation income are to be evaluated (Garnier and Ohmura, 1968). Under such circumstances, p may be evaluated from equation (3) or by using the measured value of direct radiation as an indicator of the mean atmospheric transmissivity for the day or hour in question. Both these methods require that the radiation observations being used permit direct radiation to be distinguished from sky-diffuse radiation.

Equation (4) is the fundamental equation for calculating the flux per minute of direct radiation on a surface of any slope and azimuth anywhere on earth. For practical purposes the equation must be integrated over time periods longer than the minute to which it refers. This integration can be achieved by means of a summation approximation (Ohmura, 1968) using sufficiently small time intervals (t) in the expression:

$$I_{st} = I_r \sum_{t=t_1}^{t_2} p^m \cos (\underline{X} \wedge \underline{S}) \Delta t \quad (7)$$

where I_{st} is the total over a given time period such as a day or an hour, and t_1 and t_2 are the first and last times, expressed in hour angles, when the sun shines on the surface during the period in question.

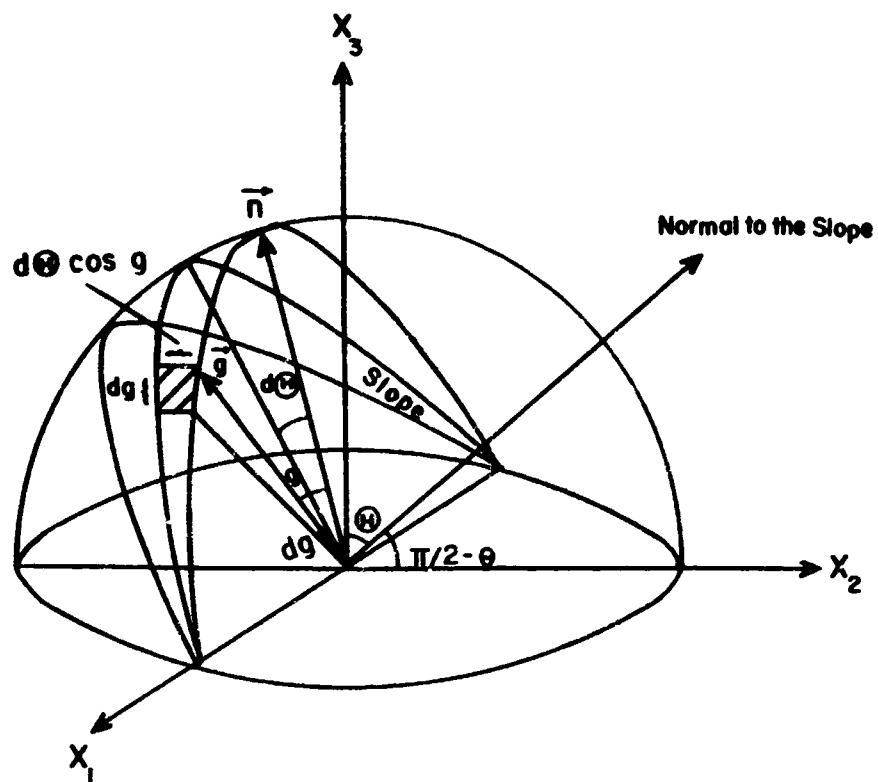


Fig. 2 The Calculation of Sky-Diffuse Radiation on a Slope

Summation at one-minute intervals is practicable with the use of high-speed computers. However, such a refinement is not normally necessary. Analysis shows that to use $t = 20$ minutes will give an accuracy, at least for daily totals, within 5% of that using $t = 1$ minute (Ohmura, 1969). Since an accuracy of 5% is within the observational error of instruments normally used for measuring radiation, such a time interval has been adopted in the calculations made in the present context.

Evaluation of Sky-Diffuse Radiation Income

The evaluation of solar radiation income is a relatively straightforward matter in that the source of origin of the radiation is a single point in the sky. When sky-diffuse radiation is considered, however, the matter becomes more complicated. Sky-diffuse radiation reaches the surface by scattering and by reflection from clouds. Under completely clear sky conditions, sky-diffuse radiation reaches the surface only by scattering, with a maximum concentration of the source of diffuse radiation in the area around the sun. The presence of clouds, however, introduces additional sources of sky-diffuse radiation until, under overcast conditions, the source of sky-diffuse radiation is a homogeneous celestial hemisphere. Under the latter conditions the scattering by water droplets will be independent of both wavelength and direction; under completely clear conditions, however, when Rayleigh scattering dominates, the flux of diffuse radiation depends both on wavelength and the direction of the ray.

It is clear from the foregoing that an almost infinite number of situations exist under which sky-diffuse radiation reaches the surface.

To solve all the cases is an almost impossible task, although the mathematical argument involved is not too complicated. This argument may be explained by reference to Fig. 2.

If the intensity of diffuse radiation from the part of the sky (g, H) is expressed as $D(g, H)$, the amount of diffuse radiation emitted from the area $\cos g \, dg \, dH$ and received on a surface, the plane of which is normal to the source of emission, will be:

$$D(g, H) \cos g \, dg \, dH$$

The flux of diffuse radiation on a slope of gradient θ will then be;

$$D(g, H) \cos^2 g \cos(H + \theta) \, dg \, dH$$

By integration it can then be shown (Ohmura, 1969) that the flux of diffuse radiation from the whole celestial hemisphere will be:

$$D_s = \int_{-\pi/2}^{\pi/2-\theta} \int_{-\pi/2}^{\pi/2} D(g, H) \cos^2 g \cos(H + \theta) \, dg \, dH \quad (8)$$

Equation (8) is thus the fundamental equation for calculating the flux of sky-diffuse radiation on a given surface. To solve it requires a large number of measurements since the value of $D(g, H)$ changes rapidly. However, if a homogeneous celestial hemisphere is assumed, equation (8) reduces (Ohmura, 1969) to the well-known Kondrat'yev equation (Kondrat'yev, 1965) for calculating the sky-diffuse radiation falling on a slope from the value measured on a horizontal surface:

$$D_s = D_h \cos^2 \frac{\theta}{2} \quad (9)$$

where D_h is the sky-diffuse radiation measured on a horizontal surface.

This equation is simple to operate and uses readily obtained data. For this reason alone it tends to be commonly used. In the present context, moreover, its use does not lead to serious inaccuracies: firstly, if the formula is used for daily totals of sky-diffuse radiation it means that there will have been integration over the entire hemisphere above the plane of the surface, so that the inaccuracies inherent in the formula will be reduced (Robinson, 1966); secondly, the contribution of sky-diffuse radiation to global radiation is minimal under clear-sky conditions when the assumption of a homogeneous celestial hemisphere is least valid, and is maximal under overcast or very cloudy conditions when calculation by the formula contributes its most accurate results. Consequently, in the present study, the topographic variations in global radiation are calculated by combining equations (4) and (9).

Accuracy of the Method of Evaluation

Theoretical considerations suggest that the procedures described for evaluating the topographic variations of global radiation income by the use of equations (4) and (9) will yield results which, at least for daily totals, do not exceed the 5% error suggested as permissible in view of instrumental limitations. To test this claim a series of measurements was made at Mont St. Hilaire, Quebec, (lat. 45°N) from August 29 to September 2, 1968*.

* A more extensive series of measurements is at present currently in progress in Barbados, but the results from them are not yet available.

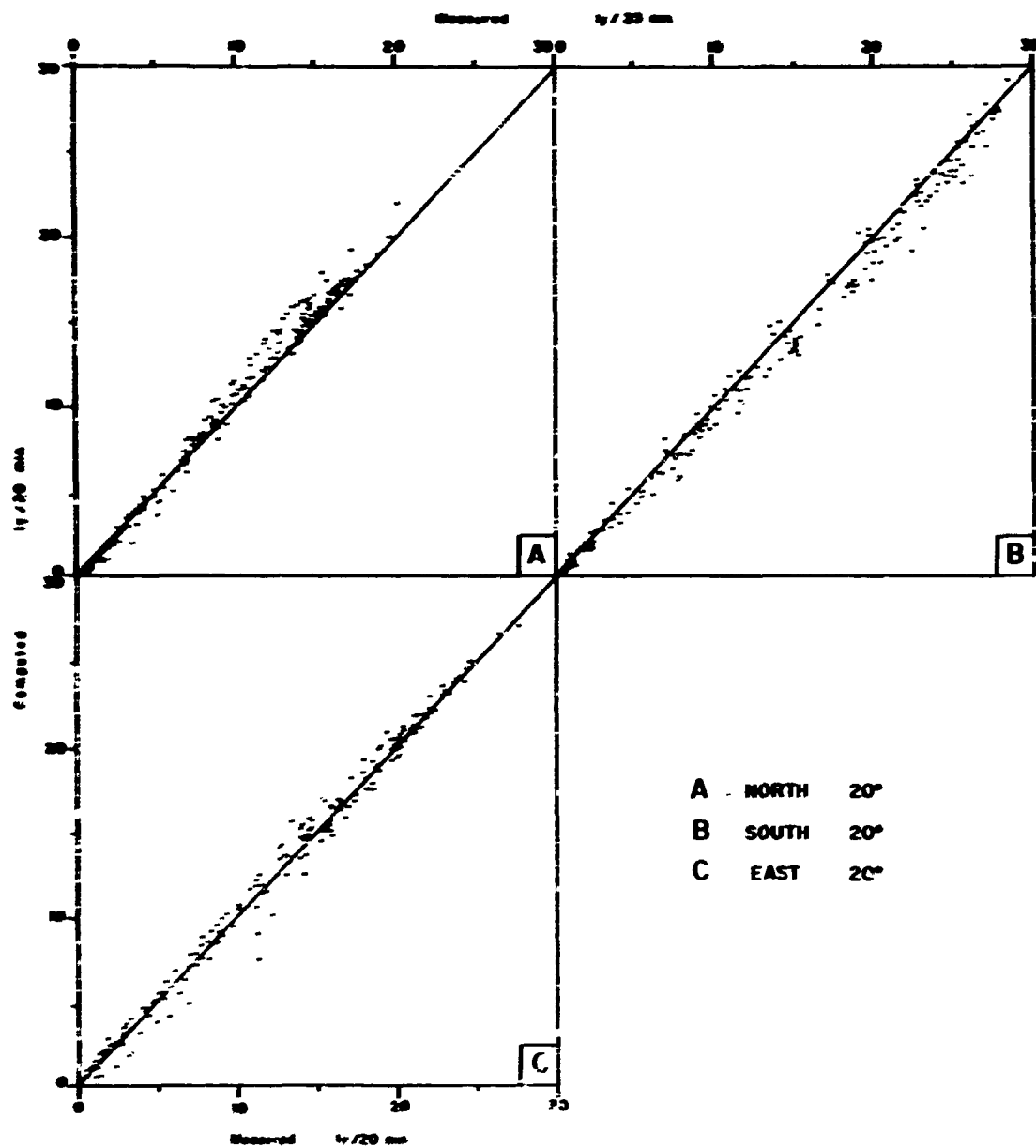


Fig. 3 Computed and Measured Values of Global Radiation, Mont St. Hilaire, Quebec (lat. 45°N), Aug. 29-Sept. 2, 1968

Three Kipp and Zonen pyranometers were installed at an angle of 20° facing north, east and south respectively. At the same time an Eppley pyranometer, tilted at an angle of 20° on a tripod and suitably shaded, was rotated successively every twenty minutes to face north, east, and south. Two other Kipp and Zonen pyranometers recorded global and sky-diffuse radiation continuously on a horizontal surface. The value of direct shortwave radiation thus evaluated for a horizontal surface was used to obtain the transmission coefficient of the atmosphere which was then employed in calculating global radiation on the sloping surfaces. For this purpose the following equation (Ohmura, 1969) was used:

$$\text{Comp. Global} = I_p^m \cos(\theta \wedge S) + D_h \cos^2 \frac{\theta}{2} + Al (Q - D_h) \sin^2 \frac{\theta}{2} \quad (10)$$

In this equation, the first and second terms on the righthand side are from equations (4) and (9). The third term is reflection from the surrounding area. Calculation shows that this third term is generally less than 3% of the shortwave reflected radiation and, therefore, contributed less than 1% of the global radiation, since the experiment was conducted in grassy surroundings where the albedo was less than 0.30. Thus, although the term was considered during the experiment its small contribution can be normally safely neglected in evaluating surface variations of short-wave radiation.

The results of the study are shown in Fig. 3. The dots are plotted in respect of the twenty minute totals computed and measured during the four days of the experiment. The 1:1 relationship line on each diagram indicates visually the resulting close correlation.

Fig. 4 Computed and Measured Values of Sky-Diffuse Radiation Values, Mont St. Hilaire, Quebec (lat. 45°N), Aug. 29 - Sept. 2, 1968

Statistically this correlation is calculated as:

North 20°	$r = 0.995$
East 20°	$r = 0.996$
South 20°	$r = 0.996$

These results suggest that the method for calculating topographic variations in short wave radiation income suggested in this report is reasonably accurate. It is interesting to note, however, that the error in calculated results is greatest on both north and south-facing slopes when measured shortwave radiation values are high, but that the sign of the error on the north slope is opposite to that on the south slope. This can be explained mainly by the formula used to evaluate sky-diffuse radiation. A comparison of the computed and measured values of this element alone is shown in Fig. 4. This comparison indicates that the two values were close to each other when the sky was overcast, and diverged considerably under clear sky conditions. Thus, when the sky is clear and the sun is high, the sky-diffuse radiation will be underestimated on a slope towards the sun owing to the high proportion of sky-diffuse radiation coming from the vicinity of the sun. For the same reason, the sky-diffuse radiation will be overestimated on a slope facing away from the sun. On the other hand, the more nearly homogeneous conditions of low sun or overcast conditions is expressed in the greater accuracy of the computed values when global radiation values are low.

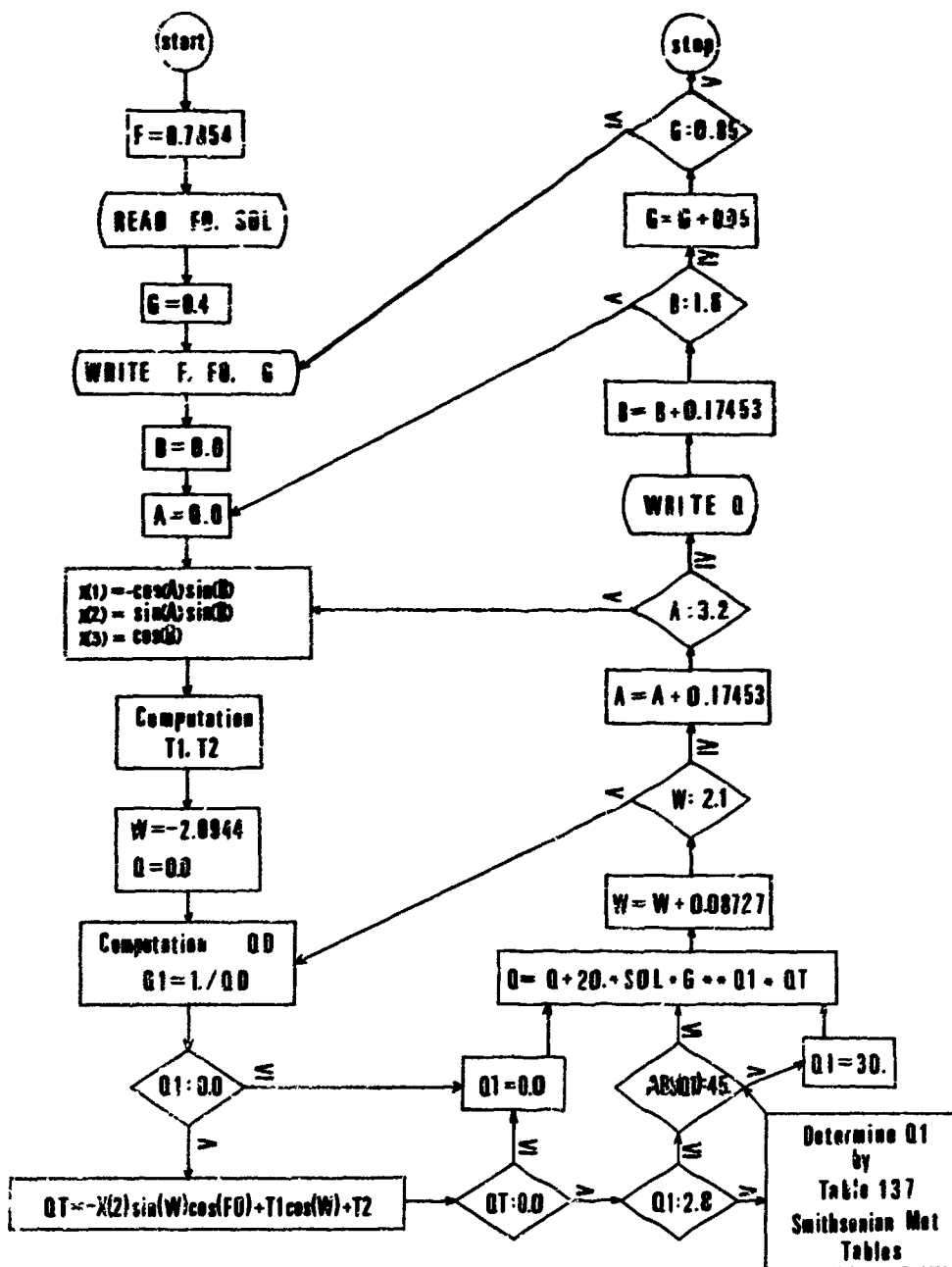


Fig. 5 The Flow Diagram for the Basic Computer Programme to Calculate Direct Radiation on a Slope

III

COMPUTER PROGRAMMING AND MAPPING PROCEDURES

The computer programming and mapping procedures whereby evaluation of surface variations of global radiation are effected may be considered in three sections: the basic computer programming involved; the way to map the data; and some particular aspects useful in a tropical context.

Basic Computer Programming

The computer programme which is fundamental to all calculation and mapping of global radiation on slopes, is the programme for computing direct radiation from equation (4), using the elements shown in equations (5) and (6) respectively. This programme, arranged for a print out in table form (Table One) is illustrated in Figs. 5 and 6.

The notation used in the programme is as follows:

- F is the latitude, given in radians.
- FO is the angle of declination of the sun, also given in radians.
- SOL is the value of the extra-terrestrial radiation in langleys per minute.
- G is the atmospheric transmissivity, given in the programme illustrated for numbers between 0.40 and 0.85 in steps of 0.05.
- Q1 is the value of the optical air mass; this is calculated from equation (6) until the sun's zenith angle is equal to 70°, from which point onwards the true optical air mass as given in the Smithsonian Meteorological Tables (List, 1966) is used.

```

C CALCULATION OF DIRECT INSOLATION ON THE SLOPES
C UNIT LANGLEYS PER DAY
0001      DIMENSION X(3), Q(19)
C LATITUDE IN RADIAN
0002      F=0.2269
C DECLINATION OF THE SUN
130 READ(5,131,END=999)FC, SCL
0003      131 FORMAT (F5.0,F4.0)
C TRANSMISSIVITY
0005      B=0.40
0006      7 WRITE (6,10) F, FC, G
0007      10 FORMAT (1H1.9H, LATITUDE#, F7.4//13H DECLINATION#, F6.2//
116+ TRANSMISSIVITY#, F5.2///
211H ANGLE OF ,45X,
3      18HAZIMUTH OF SLOPE /6H SLOPE,3X,3H 0,3X,3H 10,3X,3
4H 20,3X,3H 30,3X,3H 40,3X,3H 50,3X,3H 60,3X,
53H 70,3X,3H 80,3X,3H 90,3X,3H100,3X,3H110,3X,3H120,3X,
63H130,3X,3H140,3X,3H150,3X,3H160,3X,3H170,3X,3H180/)
0008      B=0.0
0009      BA=0.0
0010      2 A=C.0
0011      DO 1 I=1,19
0012      X(1)=-CCS(A)*SIN(B)
0013      X(2)=SIN(B)*SIN(A)
0014      X(3)=CCS(B)
0015      T1=(X(1)*SIN(F)+X(3)*CCS(F))*COS(FC)
0016      T2=(-X(1)*COS(F)+X(3)*SIN(F))*SIN(FC)
0017      W=-2.1C
0018      Q(I)=0.0
0019      5 QC=COS(FC)*CCS(F)*COS(W)+SIN(FC)*SIN(F)
0020      W=W+0.0873
0021      IF(QD.LE.0.0) GO TO 5
0022      Q2=-X(2)*SIN(W)*CCS(FC)+T1*CGS(W)
0023      CT=Q2+T2
0024      IF(W.GT.2.1) GO TO 1
0025      IF(QT.LE.0.0) GO TO 5
0026      C1=1.0/(CC+0.0001)
0027      IF(Q1-2.8) 121, 121, 122
0028      122 IF(Q1.GE.2.9) Q1=2.9C
0029      IF(Q1.GE.3.0) Q1=3.05
0030      IF(Q1.GE.3.1) Q1=3.21
0031      IF(Q1.GE.3.3) Q1=3.39
0032      IF(Q1.GE.3.5) Q1=3.59
0033      IF(Q1.GE.3.7) Q1=3.82
0034      IF(Q1.GE.4.0) Q1=4.07
0035      IF(Q1.GE.4.6) Q1=4.72
0036      IF(Q1.GE.5.0) Q1=5.12
0037      IF(Q1.GE.5.5) Q1=5.6C
0038      IF(Q1.GE.6.0) Q1=6.18
0039      IF(Q1.GE. 6.5) Q1=6.88
0040      IF(Q1.GE. 8.0) Q1=7.77
0041      IF(Q1.GE. 8.8) Q1=8.90
0042      IF(Q1.GE.10.0) Q1=10.36
0043      IF(Q1.GE.13.0) Q1=12.44
0044      IF(Q1.GE.17.0) Q1=15.36
0045      IF(Q1.GE.24.0) Q1=19.75
0046      121 IF(ABS(Q1).GT.45.0) C1=30.0
0047      Q(I)=Q(I)+20.0*SCL*G**C1*QT
0048      IF(W.LT.2.1) GO TO 5
0049      1 A=A+0.17453
0050      WRITE(6,20) BA, C
0051      20 FORMAT(20F6.1)
0052      B=B+0.17453
0053      BA=BA+10.0
0054      IF(B.LT.1.60) GO TO 2
0055      G=G+0.05
0056      IF(G.LE.0.85) GO TO 7
0057      GO TO 13C
0058      999 STCP
0059      END

```

Fig. 6 The Computer Programme to Calculate Direct Radiation on a Slope

Table One

Table of Direct Radiation on Slopes, Barbados

LATITUDE 0.2269

DECLINATION 0.40

TRANSMISSIVITY 0.65

ANGLE OF SLOPE	AZIMUTH OF SLOPE																		
	0	10	20	30	40	50	60	70	80	90	100	110	120	130	140	150	160	170	180
0.0	512.5	512.5	512.5	512.5	512.5	512.5	512.5	512.5	512.5	512.5	512.5	512.5	512.5	512.5	512.5	512.5	512.5	512.5	512.5
10.0	534.5	533.1	530.9	528.0	524.6	520.7	516.4	511.8	507.0	502.1	497.3	492.6	488.3	484.4	481.1	478.5	476.6	475.6	475.7
20.0	541.0	537.7	533.1	527.6	521.2	514.0	506.3	498.0	489.3	480.2	471.2	462.2	453.5	445.3	438.3	432.5	428.1	425.6	425.6
30.0	531.0	526.5	519.2	511.1	502.4	493.0	482.8	472.0	460.6	448.4	435.8	422.9	409.9	397.3	386.0	376.1	368.7	364.3	363.9
40.0	504.9	498.8	489.5	479.3	469.1	458.5	447.6	435.5	423.2	409.2	393.9	377.5	360.5	343.3	327.1	312.4	300.5	293.4	292.6
50.0	463.4	456.2	445.1	433.1	422.6	412.9	403.2	392.4	379.7	364.9	347.8	328.6	307.9	286.3	264.8	244.7	227.4	216.6	214.4
60.0	407.9	399.7	387.2	374.2	365.7	359.2	352.6	344.0	332.3	317.8	299.5	278.3	254.6	229.2	202.9	177.1	153.6	137.6	133.0
70.0	339.9	321.1	317.5	305.3	302.4	301.5	299.0	293.3	283.5	269.6	251.1	229.0	203.4	175.2	145.0	114.4	84.6	62.6	54.6
80.0	261.7	252.4	238.1	232.1	238.3	243.6	245.5	242.7	235.0	222.1	204.4	182.3	156.2	126.9	95.4	62.5	29.3	5.6	0.0
90.0	175.5	166.0	152.6	165.1	179.4	189.5	194.7	194.3	188.6	177.1	160.8	139.8	114.9	87.0	57.2	26.8	0.8	0.0	0.0

A and B are the azimuth and gradient of slope respectively; in the programme illustrated the azimuth is given from 0° (north) to 180° (south) in 10 degree intervals, and the slope from 0° to 90° for every 10° degree interval.

W is the hour angle expressed in radians, with solar noon equal to 0.000 radian; negative values are before noon, and positive values are after noon; in the programme illustrated calculation starts at 0400 hours and terminates at 2000 hours; the calculation is made at 20 minute intervals (20 min. = 0.873 radian).

The remaining elements of the programme constitute calculations from the formulae used to compute the surface values of direct solar radiation. These elements are found in the calculation of X(1), X(2), X(3), T1 and T2. The shadow effects taken into account are those caused by the horizon and the plane of the slope itself. In the programme, QD stands for the cosine of the sun's zenith angle. If this is negative, the sun must be

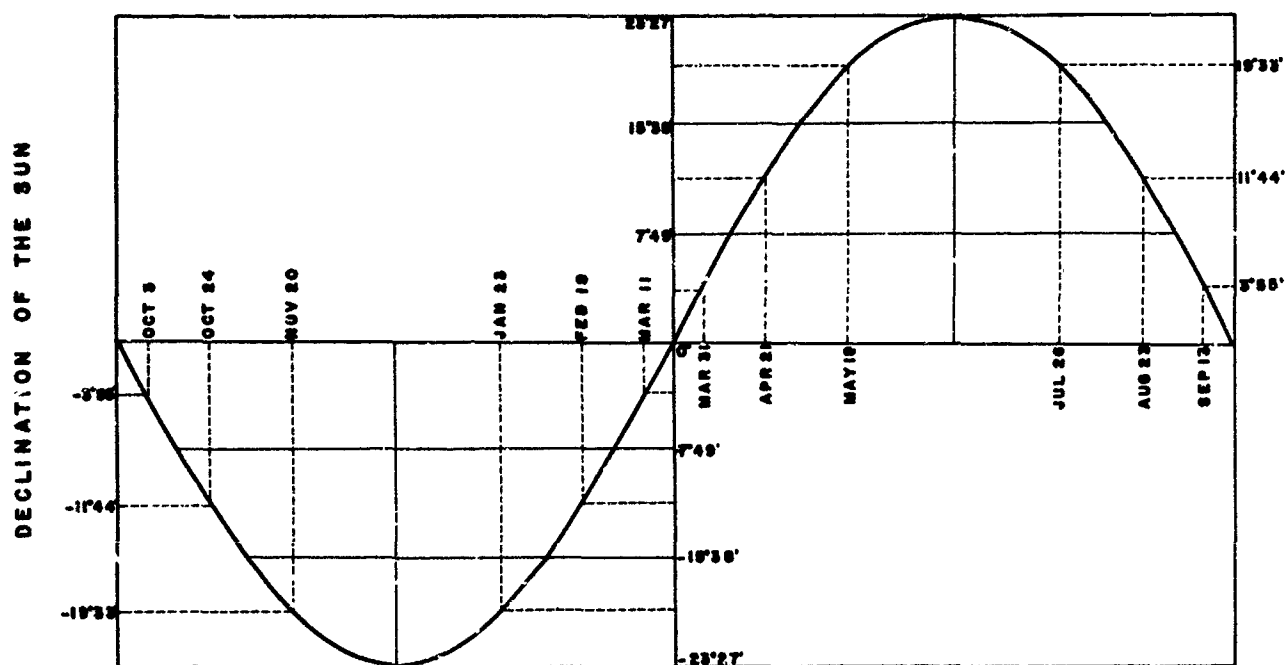


Fig. 7 Seasonal Change of the Latitude of Declination of the Sun

TABLE TWO

Solar Declinations Selected for Computer Programming

<u>Period</u>	<u>Declination</u>	<u>I_r</u> <u>(ly/min)</u>
Nov.20 - Jan.23	-23°27'	2.07
Jan.24 - Feb.18; Oct.24 - Nov. 29	-15°38'	2.06
Feb.19 - Mar.10; Oct.33 - Oct.23	-07°49'	2.04
Mar.11 - Mar.31; Sep.13 - Oct. 2	00°00'	2.02
Apr. 1 - Apr.21; Aug.23 - Sep.12	07°49'	1.99
Apr.22 - May 18; Jul.26 - Aug.22	15°38'	1.97
May 19 - Ju. 25	23°27'	1.94

below the horizon. QT denotes the cosine of the angle between the normal of the slope and the direction of the sun. QT will be negative when the sun is behind the slope. Thus, by eliminating QD when negative and QT when negative from the accumulation of the values computed every twenty minutes, it becomes unnecessary to determine the hours when the sun shines for the first time (t_1 in equation (7)), and the last time (t_2 in equation (7)) on each slope.

It is apparent that the computer programme illustrated applies to a particular latitude (F) and refers also to a given time period for which the angle of declination of the sun (FO) and the extra-terrestrial radiation (SOL) remain constant. The value of the latitude remains a constant which fixes the location of the area being examined. The values of FO and SOL , however, will vary during the year.

To take account of the changes in FO and SOL for each day or week of the year is time consuming and, in practice, unnecessary since the influence of the day to day changes in the sun's position in equation (7) is insignificant as compared with the influence of the other terms. Thus, it is convenient to divide the year into periods for which a suitable declination and value of extra-terrestrial radiation can be used. Since the curve of the latitude of the sun's declination against time is sine-like, the procedure followed has been to divide the year into periods of unequal length for which a given declination and value of I_r can be regarded as a true mid-value. Such a division is given in Fig. 7 and Table Two. The length of the periods have been chosen bearing in mind the earlier stipulation that an accuracy of 5% is appropriate in view of instrumental limitations. A division of the year into twelve periods has, accordingly, been made, centering upon

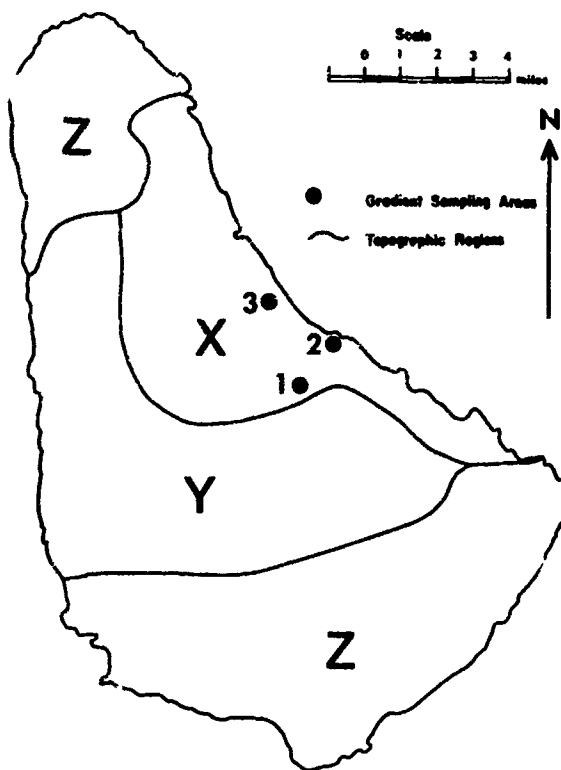


Fig. 8 Regions of Barbados for Relief Sampling
 X: Complicated relief; Y: Intermediate relief;
 Z: Gentle relief

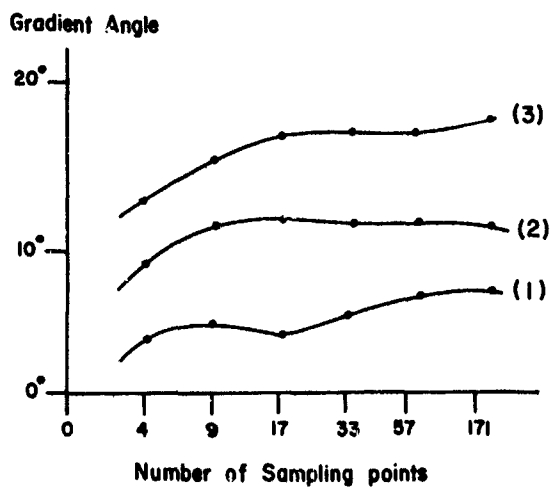


Fig. 9 Sampling Points and Gradient Angles for the
 Radiation Mapping Grid of Barbados

NOTE: Bracketed numbers refer to the sampling areas
 in Fig. 8

the representative declination and values of I_r given in Table 2.

Mapping the Data

In order to map the topographic variations in short wave radiation over a given area an appropriate base map must be prepared. This involves covering the area of study with a grid at each intersection of which is marked the azimuth and gradient of slope. The closeness of the grid must be decided in terms of the detail of the study being made and also the intensity of the relief of the area.

The grid system used for the map of Barbados appearing in this report was made from the eighteen sheets of the 1:10,000 topographic series, prepared in 1953 by the British Colonial Surveys (Basnayake, 1968). These map sheets have on them a basic grid, 10 cm square. This grid provided a sufficiently close network for the southern half of the island, with its gently-rolling physiography. The more hilly central and eastern parts of Barbados, however, required a closer grid system.

To determine this detail, three 10 cm squares of varying types of complicated relief were selected (Fig. 8). The average gradient for each square was calculated using successively doubled numbers of sampling points. The results are shown in Fig. 9. The gradient averages reached stable values at between 17 and 33 points per 10 cm square. Therefore, the figure of 25 points per 10 cm square was chosen for the areas of most complicated relief of the island. This resulted in a grid pattern of 2.5 cm squares.

An identical procedure was adopted as a means of selecting

the grid density for use in areas of intermediate relief. As a result a grid of 5 cm squares was adopted for this part of the island. Thus, it was possible to divide the island into the three regions shown in Fig. 8.

To measure the gradient of the slope at each point of the resulting grid, the number of successive contour lines over standard distance was used rather than the difference between individual adjacent contours. This procedure was followed for two reasons: it is easier to count the successive contours over a comparatively large pre-determined standard distance than to measure accurately small distances between two contours; and to use a standard distance for gradient measurement enables an average value to be obtained that takes into account the area around a sampling point, rather than using the value at a given single point. A circle, 15 mm in diameter, was used for gradient analysis. This proved to be an optimum size which avoided both the ambiguity of single contour interpretation arising from the use of a smaller circle, and the difficulty of determining average slope direction and counting too many contours if a larger circle were used.

The 1:10,000 maps used to prepare the base map have contours on them at 20 ft. intervals. For such a map, therefore, the number of contours in a 15 mm distance corresponding to different angles of slope is given by,

$$Y = \frac{15 \tan X}{0.610} \quad (11)$$

where X is the given angle of slope and Y the number of contour crossings in 15 mm of map distance.

The calculation of the values of azimuth and gradient to be

inserted at each intersection of the grid was effected by means of a clear plastic protractor, with a movable pointer of semi-rigid clear plastic pivoted at the origin of the protractor. The pointer was marked with a central longitudinal line, with another line at right-angles to it and passing through the pivoted origin. A circle of 15 mm diameter, with its centre at the pivoted origin, was also marked on the pointer. The protractor, with the pointer attached, was placed with its centre of origin on the selected grid intersection of the topographic map. To obtain the azimuth of the slope, the pointer was moved so that its marker line was perpendicular to the major contour trend, and the appropriate angle was then read on the circular margin of the protractor. For gradients, it was simply necessary to count the successive contours within the 15 mm circle and to read the corresponding gradient from the values in a table prepared from equation (11).

When measuring the gradients care was taken to ensure that the contour lines were truly successive, and were not repeating the same values as, for example, in the case of those doubling back on themselves. In the case of open valleys or spurs, slope measurement was done on the main axis. Narrow, deep valleys, a large number of which exist in the limestone topography of Barbados, were ignored in the slope analysis. This was because, in general, they play an insignificant role in the regional picture of surface radiation variation, and especially because many of them were found, on inspection in the field, to be choked with bushes and trees so that the effective surface was often level with the adjacent surroundings, if not actually higher.

To effect the mapping of global radiation by using the base map prepared in this way, a computer programme was made which calculated

the value of the global radiation for each intersection of the base-map grid. This calculation is made from the radiation data of a single, representative site, which, in the case of the maps appearing in this report, constitute the observations of global and sky-diffuse radiation made in 1964 at the Brace Experiment Station, in the grounds of the Bellairs Research Institute, St. James (Tout, 1967, 1968).

For mapping purposes two sets of data cards were prepared: one showing the azimuth and the other showing the gradient for each intersection of the base-map grid. The maximum possible number of columns per card for this purpose was twenty, since four units are needed to indicate the azimuth in degrees and whether it is positive or negative. Thus, the grid covering Barbados was grouped suitably into major divisions, each division being twenty grid-points wide. The programme thus calculated the global radiation values at the grid points in one continuous length, twenty columns wide. The resulting print-out was then divided suitably so as to conform to its actual pattern on the map. To ensure the correlation of points on the map, an appropriate overlap was made in the division of the grid into twenty-column-wide units.*

The calculations effected by the computer are illustrated in Fig. 10. The latitude (F) is expressed in radians. After reading the cards giving the azimuth and gradient of each point in degrees, the values at these points are converted into radians in steps 12 and 13. Step 15 reads the year, month, and day ($L1$), the declination of the sun

* In practice, it was found convenient to confine the division into twenty columns to the region of complicated relief on the island. The remainder of the island, where the base grid was wider, was divided into fourteen column-wide units, and the computer programming for calculating this part of the island was modified accordingly.

```

0001      C  GLOBAL RADIATION MAP BARBADOES
          DIMENSION A(120,20),B(120,20),X(3),S(120,20)
0002      C  INPUT LATITUDE IN RADIANS
          F=C.2269
0003      C  READ THE NUMBER OF CARDS
          READ(5,888) L
0004      888 FORMAT(I3)
          C  READ AZIMUTH AND GRADIENT OF SLOPES
0005      READ(5,100) ((A(I,J), J=1,20), I=1,L)
0006      100 FORMAT (20F4.0)
0007      READ(5,101) ((B(I,J), J=1,20), I=1,L)
0008      101 FORMAT (20F5.0)
0009      DO 880 I=1,L
0010      DO 880 J=1,20
0011      IF(B(I,J).EC.90.C) GO TO 880
0012      A(I,J)=A(I,J)*0.C1745
0013      B(I,J)=B(I,J)*0.C1745
0014      880 CONTINUE
0015      661 READ(5,102,END=999)L1, FC, IF, CIR, CIF
0016      102 FORMAT(I2, F4.0, I2, 2F6.C)
0017      WRITE (6,556)
0018      556 FORMAT (1H1)
0019      WRITE (6,103)L1, FC, IF, CIR, CIF
0020      103 FORMAT(4H DATE# , 18, 13H CECLINATION# ,F4.C, 12//19H DIRECT INSOL
          IATION# ,F6.1/24H SKY-DIFFUSE INSOLATION# ,F5.1)
0021      FIF=IF
0022      FIF=FIF*0.0167
0023      IF(FO) 20, 20, 21
0024      20 FC=(FC-FIF)*0.01745
0025      GO TO 22
0026      21 FC=(FC+FIF)*0.01745
0027      22 G=0.50
0028      154 SS=0.0
0029      W=-2.16
0030      155 CD=COS(FC)*COS(F)*COS(W)*SIN(FO)*S A(F)
0031      Q1=1.0/(CD+0.0001)
0032      IF(ABS(Q1).GT.40.0) Q1=30.C
0033      IF(QD.LT.0.0) CD=0.0
0034      SS=SS+80.0*G**Q1*CD
0035      W=W+0.1746
0036      IF(W.LT.2.2) GO TO 155
          C  COMPARISON BETWEEN CIR AND SS
0037      D=CIR-SS
0038      IF(ABS(D)- 5.0) 162, 162, 161
0039      161 IF(DIR.GT.SS) GO TO 163
0040      G=G-0.C5
0041      GO TO 154
0042      163 G=G+0.C15
0043      GO TO 154
0044      162 WRITE (6, 171) G
0045      171 FORMAT(17H TRANSMISSIVITY# , F5.4//)
0046      DO 778 I=1,L
0047      DO 778 J=1,20
0048      IF(B(I,J).EC.90.) GO TO 414

```

Fig. 10 The Computer Programme for Calculating
Global Radiation over Barbados

(continued over page).

```

0049      X(1)=-COS(A(I,J))*SIN(B(I,J))
0050      X(2)=SIN(B(I,J))*SIN(A(I,J))
0051      Y(3)=CCS(B(I,J))
0052      T1=(X(1)*SIN(F)+X(3)*CCS(F))*CCS(F)
0053      T2=(-X(1)*COS(F)+X(3)*SIN(F))*SIN(F)
0054      W=-2.16
0055      S(I,J)=0.0
0056      5 QQ=COS(FC)*COS(F)*CCS(W)+SIN(FC)*SIN(F)
0057      Q1=1.0/(C0+0.0001)
0058      IF(Q1-2.0) 121, 121, 122
0059      122 IF(Q1.EE.2.9) Q1=2.90
0060      IF(Q1.EE.3.0) Q1=3.05
0061      IF(Q1.EE.3.1) Q1=3.21
0062      IF(Q1.EE.3.3) Q1=3.36
0063      IF(Q1.EE.3.5) Q1=3.59
0064      IF(Q1.EE.3.7) Q1=3.82
0065      IF(Q1.EE.4.0) Q1=4.07
0066      IF(Q1.EE.4.6) Q1=4.72
0067      IF(Q1.EE.5.0) Q1=5.12
0068      IF(Q1.EE.5.5) Q1=5.60
0069      IF(Q1.EE.6.0) Q1=6.18
0070      IF(Q1.EE. 6.5) Q1=6.88
0071      IF(Q1.EE. 8.0) Q1=7.77
0072      IF(Q1.EE. 8.0) Q1=8.90
0073      IF(Q1.EE.10.0) Q1=10.35
0074      IF(Q1.EE.13.0) Q1=12.44
0075      IF(Q1.EE.17.0) Q1=15.36
0076      IF(Q1.EE.24.0) Q1=19.75
0077      121 IF(ABS(Q1)-67.45.0) Q1=30.0
0078      Q2=-X(2)*SIN(W)*CCS(F)+T1*CCS(W)
0079      QT=Q2+T2
0080      IF(QC.LT.0.0.OR.CT.LT.C.C) QT=C.C
0081      S(I,J)=S(I,J)+80.0*G**Q1*QT
0082      W=W+0.1745
0083      IF(W.LT.2.2) GC TO 5
0084      S(I,J)=S(I,J)+DIF*(CCS(B(I,J)/2.0))*2
0085      GO TO 778
0086      414 S(I,J)=0.0
0087      778 CONTINUE
0088      WRITE (6,632) ((S(I,J), J=1,20), I=1,L)
0089      632 FORMAT(2CF5.0)
0090      GO TO 661
0091      999 STOP
0092      END

```

Fig. 10 (Continued)

(FO, IF), and the direct (DIR) and sky-diffuse (DIF) radiation for the day in question. The declination of the sun is expressed in degrees (FO) and minutes (IF), and this value is converted to radians in steps 21 to 26. The direct and sky-diffuse radiation are daily totals in langleys. Thus the programme can be used for a particular day, or else for a longer period by using the mean daily value for the period in question. Steps 28 to 43 effect the calculation of atmospheric transmissivity (G). This is achieved by first calculating a daily total (SS) on the basis of a transmissivity of 0.50 and accumulations every 40 minutes. This total is then compared with the direct radiation total already supplied, and a re-calculation altering the value of G, either by decreasing it (step 40) or increasing it (step 42), effected until the value of SS is within 5 langleys of the value of measured direct radiation. The value of G which achieves this is then used to calculate the direct radiation at each grid point in a manner similar to that already explained in connection with the base programme. The contribution of sky-diffuse radiation is added in step 84.

The programme illustrated in Fig. 10 is arranged for a print-out in table form (Fig. 11). This print-out gives the values of global radiation at each grid intersection of the base map. Plotting the data and drawing the relevant isarithms by hand thus becomes routine cartographic procedure. Although this perhaps sounds an unnecessarily lengthy way to produce the final map in view of the availability of computer mapping programmes, in fact it was found the most appropriate way for making the maps of Barbados. This conclusion was reached after trying out the computer mapping programme illustrated in Fig. 12.

506.	525.	525.	525.	0.	C.	0.	0.	0.	0.	0.	0.	0.	0.	0.	0.	0.	0.	0.
506.	535.	525.	525.	C.	C.	0.	C.	0.	C.	0.	0.	0.	0.	0.	0.	0.	0.	0.
384.	446.	518.	525.	525.	C.	0.	C.	0.	C.	0.	0.	0.	0.	0.	0.	0.	0.	0.
608.	637.	506.	525.	525.	C.	0.	C.	0.	C.	0.	0.	0.	0.	0.	0.	0.	0.	0.
525.	525.	525.	525.	525.	525.	0.	C.	0.	C.	0.	0.	0.	0.	0.	0.	0.	0.	0.
525.	525.	525.	525.	489.	431.	490.	0.	0.	0.	0.	0.	0.	0.	0.	0.	0.	0.	0.
477.	506.	5.5.	525.	524.	503.	500.	525.	0.	C.	0.	0.	0.	0.	0.	0.	0.	0.	0.
592.	525.	513.	472.	433.	382.	424.	44C.	525.	0.	0.	0.	0.	0.	0.	0.	0.	0.	0.
525.	513.	455.	394.	263.	468.	450.	515.	525.	C.	0.	0.	0.	0.	0.	0.	0.	0.	0.
525.	509.	418.	503.	424.	446.	605.	534.	343.	477.	0.	0.	0.	0.	0.	0.	0.	0.	0.
49C.	518.	410.	516.	523.	482.	495.	574.	516.	455.	0.	0.	0.	0.	0.	0.	0.	0.	C.
535.	486.	545.	455.	598.	417.	519.	487.	397.	446.	500.	0.	0.	0.	0.	0.	0.	0.	0.
497.	486.	513.	473.	468.	451.	445.	417.	585.	537.	490.	525.	0.	0.	0.	0.	0.	0.	0.
495.	531.	571.	565.	558.	491.	473.	473.	481.	446.	440.	463.	525.	0.	0.	0.	0.	0.	0.
494.	434.	538.	564.	620.	505.	433.	445.	463.	456.	489.	431.	451.	525.	0.	0.	0.	0.	0.
394.	454.	470.	450.	462.	505.	494.	477.	338.	434.	358.	558.	556.	463.	0.	0.	0.	0.	0.
494.	417.	445.	513.	443.	413.	455.	474.	586.	55C.	506.	446.	491.	481.	500.	0.	0.	0.	0.
520.	519.	495.	413.	362.	321.	445.	506.	434.	446.	384.	474.	400.	446.	485.	487.	525.	0.	0.
516.	522.	459.	518.	589.	545.	634.	585.	630.	577.	619.	547.	506.	441.	418.	464.	463.	525.	0.
487.	476.	463.	45C.	565.	535.	57C.	605.	600.	654.	608.	619.	589.	619.	525.	531.	464.	463.	470.
383.	57C.	590.	547.	440.	44C.	624.	512.	600.	603.	525.	525.	491.	455.	488.	488.	445.	464.	451.
472.	444.	516.	402.	357.	598.	558.	536.	470.	462.	487.	378.	462.	455.	428.	455.	497.	471.	418.
576.	434.	413.	402.	585.	592.	471.	474.	471.	487.	433.	408.	428.	445.	441.	445.	471.	445.	433.
408.	440.	488.	474.	477.	485.	485.	510.	445.	462.	429.	449.	464.	449.	354.	258.	394.	427.	417.
339.	494.	449.	495.	462.	441.	535.	445.	445.	384.	494.	433.	433.	378.	525.	464.	408.	307.	417.
474.	413.	560.	455.	440.	532.	488.	462.	446.	429.	445.	482.	338.	525.	451.	357.	429.	536.	525.
538.	543.	580.	506.	533.	486.	428.	450.	446.	433.	400.	429.	514.	525.	536.	536.	539.	530.	539.
494.	520.	565.	497.	556.	464.	428.	445.	563.	536.	525.	535.	539.	559.	539.	539.	539.	538.	539.
513.	523.	491.	506.	455.	511.	525.	554.	525.	536.	555.	555.	539.	539.	539.	571.	539.	538.	536.
560.	551.	539.	525.	560.	555.	574.	555.	574.	574.	555.	539.	539.	572.	571.	571.	525.	538.	525.
525.	0.	0.	C.	0.	C.	0.	0.	0.	0.	0.	0.	0.	0.	0.	0.	0.	0.	0.
477.	445.	485.	47C.	0.	0.	0.	C.	0.	C.	0.	0.	0.	C.	0.	0.	0.	0.	0.
402.	481.	448.	477.	445.	428.	525.	C.	0.	C.	0.	0.	0.	0.	C.	0.	0.	0.	0.
455.	445.	455.	445.	433.	477.	477.	C.	0.	C.	0.	0.	0.	0.	0.	0.	0.	0.	0.
418.	473.	441.	477.	441.	464.	431.	455.	0.	0.	0.	0.	0.	0.	0.	0.	0.	0.	0.
391.	477.	464.	445.	563.	446.	446.	47C.	431.	525.	C.	0.	0.	0.	0.	0.	0.	0.	0.
310.	339.	408.	455.	418.	481.	474.	47C.	491.	483.	525.	0.	0.	0.	0.	0.	0.	0.	0.
536.	536.	525.	361.	441.	361.	408.	418.	445.	497.	497.	506.	509.	440.	483.	0.	0.	0.	0.
539.	539.	539.	525.	538.	397.	418.	431.	477.	418.	487.	448.	400.	491.	525.	525.	0.	0.	0.
536.	525.	539.	538.	549.	535.	525.	481.	446.	418.	400.	477.	491.	518.	525.	523.	525.	0.	0.
530.	525.	525.	538.	549.	513.	537.	417.	379.	417.	400.	506.	542.	512.	455.	455.	486.	455.	525.
0.	0.	0.	C.	0.	C.	0.	0.	525.	477.	455.	463.	483.	417.	487.	497.	513.	525.	525.
0.	0.	0.	0.	0.	C.	0.	0.	517.	418.	400.	430.	490.	485.	417.	463.	474.	515.	500.
0.	0.	0.	0.	0.	C.	0.	0.	0.	0.	543.	431.	464.	408.	365.	474.	446.	477.	491.
0.	0.	0.	C.	0.	C.	0.	C.	0.	0.	525.	525.	530.	525.	464.	519.	519.	455.	477.
0.	0.	0.	0.	0.	C.	0.	C.	0.	C.	0.	0.	0.	0.	525.	518.	491.	440.	497.
0.	0.	0.	0.	0.	C.	0.	0.	0.	0.	0.	0.	0.	0.	533.	533.	523.	481.	497.
0.	0.	0.	0.	0.	C.	0.	0.	0.	0.	0.	0.	0.	0.	0.	0.	525.	525.	463.
0.	0.	0.	0.	0.	C.	0.	0.	0.	C.	0.	0.	0.	0.	0.	0.	525.	525.	525.
0.	0.	0.	0.	0.	C.	0.	0.	0.	0.	0.	0.	0.	0.	0.	0.	525.	525.	506.
0.	0.	0.	0.	0.	C.	0.	0.	0.	0.	0.	0.	0.	0.	0.	0.	525.	525.	514.

Fig. 11 A Sample of Global Radiation Values,
Barbados

```

0001      C RADIATION STUDY, GLOBAL RADIATION MAP, BARBADOS.
          DIMENSION A(120,20),B(120,20),X(3),E(96),SYMBOL(50),S(120,20),C(4,
          196)
0002      C INPUT LATITUDE IN RADIAN.
          F=0.2269
0003      C READ GRAPHING SYMBOLS
          READ (5,700) (SYMBOL(I),I=1,50)
0004      700 FORMAT (50A1)
          C READ THE LENGTH OF THE MAP
0005      READ(5,888) L
0006      888 FORMAT(I3)
0007      LL=L-1
          C READ AZIMUTH AND GRADIENT OF SLOPES
0008      READ(5,100) ((A(I,J), J=1,20),I=1:L)
0009      100 FORMAT (20F4.0)
0010      READ(5,101) ((B(I,J),J=1,20), I=1,L)
0011      101 FORMAT (20F3.0)
0012      DO 880 I=1,L
0013      DO 880 J=1,20
0014      IF(B(I,J).EQ.90.0) GO TO 880
0015      A(I,J)=A(I,J)*0.01745
0016      B(I,J)=B(I,J)*0.01745
0017      880 CONTINUE
0018      661 READ(5,102,END=556) L1, FC, IF, DIR, CIF
0019      102 FORMAT(I8, F4.0, I2, 2F6.0)
0020      WRITE (6,556)
0021      556 FORMAT (1H1)
0022      WRITE (6,103) L1, FO, IF, CIF, CIF
0023      103 FORMAT(6H DATE# , I8, 13H DECLINATION# ,F4.0, 12//19H DIRECT INSOL
          IATION# ,F6.1/24H SKY-DIFFUSE INSCLATION# ,F5.1)
0024      FIF=IF
0025      FIF=FIF*0.0167
0026      IF(FO) 20, 20, 21
0027      20 FC=(FC-FIF)*0.01745
0028      GO TO 22
0029      21 FC=(FC+FIF)*0.01745
0030      22 G=0.50
0031      154 SS=0.0
0032      W=-2.16
0033      155 QD=CCS(FC)*CCS(F)*COS(W)+SIN(FC)*SIN(F)
0034      Q1=1.0/(QD+0.0001)
0035      IF(ABS(Q1).GT.40.0) C1=30.0
0036      IF(QD.LT.0.0) QD=0.0
0037      SS=SS+FO.0*G**Q1*QD
0038      W=W+0.1746
0039      IF(W.LT.2.2) GO TO 155
          C COMPARISON BETWEEN DIR AND SS
0040      C=DIR-SS
0041      IF(ABS(C)- 5.0) 162, 162, 161
0042      161 IF(DIR.GT.SS) GO TO 163
0043      G=0.05
0044      GO TO 154
0045      163 C=G+0.015
0046      GO TO 154
0047      162 WRITE (6, 171) G
0048      171 FORMAT(17H TRANSMISSIVITY# , F5.4//)
0049      DO 770 I=1,L
0050      DO 770 J=1,20
0051      IF(B(I,J).EQ.90.0) GO TO 414
0052      X(1)=-CCS(A(I,J))*SIN(B(I,J))
0053      X(2)=SIN(P(I,J))*SIN(A(I,J))
0054      X(3)=CCS(B(I,J))
0055      T1=(X(1)*SIN(F)+X(3)*COS(F))*CCS(FO)
0056      T2=(-X(1)*COS(F)+X(3)*SIN(F))*SIN(FO)
0057      W=-2.16
0058      S(I,J)=C.0

```

Fig. 12 Computer Programme to Map Global Radiation, Barbados

(continued over page).

```

0054      5 GC=CCS(FC)+CCS(F)*CCS(h)+SIN(FC)*SIN(F)
0060      Q1=1.0/(CD+0.0001)
0061      IF(Q1-2.8) 1,1, 121, 122
0062      122 IF(J1,CF,2.9) C1=2.90
0063      IF(Q1,CF,3.0) C1=3.05
0064      IF(Q1,CF,3.1) C1=3.21
0065      IF(Q1,CF,3.3) C1=3.35
0066      IF(Q1,CF,3.5) C1=3.55
0067      IF(Q1,CF,3.7) C1=3.82
0068      IF(Q1,CF,4.0) C1=4.07
0069      IF(Q1,CF,4.6) C1=4.77
0070      IF(Q1,CF,5.0) C1=5.12
0071      IF(Q1,CF,5.5) C1=5.45
0072      IF(Q1,CF,6.0) C1=6.18
0073      IF(Q1,CF, 6.5) C1=6.88
0074      IF(Q1,CF, 8.0) C1=7.77
0075      IF(Q1,CF, 8.8) C1=8.50
0076      IF(Q1,CF,10.0) C1=10.35
0077      IF(Q1,CF,13.0) C1=12.44
0078      IF(Q1,CF,17.0) C1=15.36
0079      IF(Q1,CF,24.0) C1=19.75
0080      121 IF(ABS(C1)-GT,45.0) C1=30.0
0081      Q2=-X(2)*SIN(h)*CCS(FC)+T1*CCS(h)
0082      CT=J2+T2
0083      IF(UC,LT,0.0,OH,LT,LT,C,C) LT=0.0
0084      S(I,J)=S(I,J)+HC,0*G=C1*CT
0085      h=h+0.1745
0086      IF(h,LT,2.2) GC TC 5
0087      S(I,J)=S(I,J)+DIF*(CCS(R(I,J)/2.0))**2
0088      GC TC 778
0089      414 S(I,J)=0.0
0090      778 CONTINUE
C EXPAND THE ARRAY INTO 4,56
0091      LA=1
0092      801 DO HOC I=LA,LA
0093      DO 800 J=1,20
0094      C(I,J*5-4)=S(I,J)
0095      800 C(I,J*5-4)=S(I+1,J)
0096      DO 777 I=1,4,3
0097      DO 777 J=1,91,5
0098      DO 777 M=1,4
0099      CM=M
0100      777 C(I,J+M)=((5.0-CM)*C(I,J)+CM*C(I,J+5))/5.0
0101      DO 111 I=1,1
0102      DO 111 J=1,96
0103      DO 111 N=1,2
0104      CN=N
0105      111 C(I+N,J)=((3.0-CN)*C(I,J)+CN*C(I+3,J))/3.0
0106      I=1
0107      602 DO 701 J=1,96
0108      K=C(I,J)/25.0+1.0
0109      F(J)=SYMBOL(K)
0110      701 CONTINUE
0111      WRITE(6,704) F
0112      704 FORMAT(1H,56A1)
0113      I=I+1
0114      IF(I,LE,3) GC TC 602
0115      LA=LA+1
0116      IF(LA,LE,LL) GC TO 801
0117      GC TC 661
0118      999 STOP
0119      END

```

TOTAL MEMORY REQUIREMENTS 008488 BYTES

Fig. 12 (Continued)

The print-out for this programme (Fig. 13) uses a symbolism based on an isarithmic interval of 25 langleys. The arrangement of this symbolism is based on groups of three letters separated by blanks. Since daily totals of global radiation are unlikely to be below 100 langleys in the tropics, the first symbol (*) indicates a range of 75-100 langleys. The other values then follow by letters of the alphabet:

* ABC DEF GHI JKL MNO PQR STU

From this sequence it follows that A refers to 125-149 langleys, B to 150-174 langleys, C to 175-199 langleys, the blank between C and D to 200-224 langleys, and so on. The plotting scale on the computer map is half-an-inch between each grid point, and the computer effects an interpolation between the calculated values at each of these points.

A sample of a map of part of Barbados prepared in this way, with isarithms drawn in by hand, is given in Fig. 13. The map illustrates the advantages of the system as a rapid means of providing a general picture of the distribution. For a map of the whole of Barbados, however, modification of the programme is necessary in view of the different density of grid points used to sample the varied topography of the island, or alternatively a rather complicated arrangement of enlargement and reduction of the maps of different regions has to be done to bring them together on one, suitable scale. Even with such modifications, all of which were tested, the resulting map presented a rather generalized picture. After a number of trials of different systems, therefore, it was decided to use the digital print-out illustrated in Fig. 10 as the most appropriate method for preparing the maps illustrated in this report.

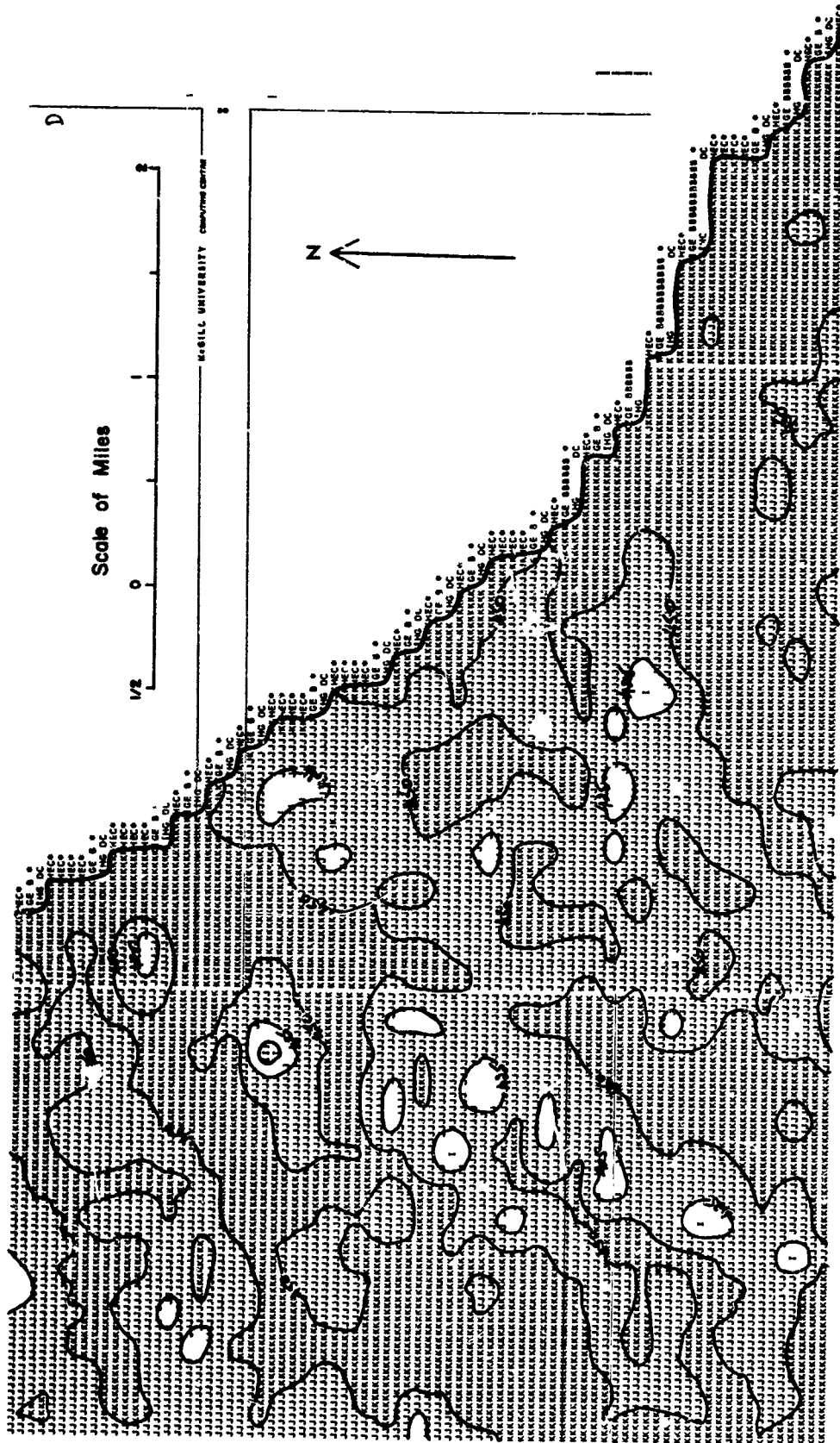


Fig. 17 Sample of a Computer-Produced Map of Global Radiation over part of Barbados

Hourly Radiation Mapping

Although the method for evaluating the surface variations of global radiation which has been outlined is intended primarily for use with daily totals or longer periods, the tests for accuracy given to the system at Mont St. Hilaire, Quebec, suggest that it can, in fact, be used for shorter periods, with probably an hour as the minimum reliable time period. It is useful in the tropics to examine the radiation distribution over such a short period. This is because the sun rises quickly and its heating effects are strong soon after sunrise and until just before sunset. By the time the sun has reached an altitude of 30° above the horizon topographic influences become somewhat reduced. The varied pattern of heating in the early morning hours, however, can theoretically influence the development of early morning convection. In Barbados the steepest slopes on the island tend to be generally towards the east. Thus, it was felt desirable to arrange a computer programme to calculate the topographic variations of global radiation on an hourly basis.

Such a programme is illustrated in Fig. 14. It is basically the same as those shown in Figs. 10 and 12, but differs somewhat in the data supplied to it. These data are indicated in step 15 of Fig. 14. They consist of the year, month, and day (L1), the angle of declination of the sun (FO, IF), the extra-terrestrial radiation (SOL) in langleys per minute, the atmospheric transmissivity (G) for the hour in question, the sky-diffuse radiation in langleys for the hour (DIF), and the time, which is given as an hour angle in degrees and decimals of a degree, with solar noon as zero and negative values before noon. This time value

```

0001 C PARLAT (1) STUDY OF PARADES HCOFLY MAPPING
      DIMENSION A(120,20),B(120,20),X(3),S(120,20)
0002 C IMPLT LATITUDE IN PACIANS
      F=C.2269
0003 C READ THE NUMBER OF CARDS
      RFAC(5,888) L
0004 888 FCFMAT(13)
0005 C REA. AZIMUTH AND GRADIENT OF SLOPES
      READ(5,100) ((A(I,J), J=1,20), I=1,L)
0006 100 FCFMAT (2CF4,0)
0007 RFAC(5,101) ((B(I,J),J=1,20), I=1,L)
0008 101 FCFMAT (2OF3,0)
0009 DO 880 I=1,L
0010 DO 880 J=1,20
0011 IF(B(I,J).EQ.90.0) GO TO 880
0012 A(I,J)=A(I,J)*0.01745
0013 B(I,J)=B(I,J)*0.01745
0014 880 CONTINUE
0015 661 RFAC(5,102,END=999) L1, FC, IF, SCL, G, DIF, TIME
0016 102 FCFMAT(18, F4.0, 12, 4F6.0)
0017 N=TIME*0.01745
0018 WRITE (6,956)
0019 956 FCFMAT (1H1)
0020 WRITE(6,103) L1,FC, IF, G, DIF, TIME
0021 103 FCFMAT(6H DATE# , 18, 13H DECLINATION# ,F4.0, 12//17H TRANSMISSIVI
      TY# ,F6.3/24H SKY-DIFFUSE INSOLATION# ,F5.1/6H TIME# ,F6.2)
0022 FIF=IF
0023 FIF=FIF*C.0167
0024 IF(FC) 20, 20, 21
0025 20 FC=(FC-FIF)*C.01745
0026 GO TO 162
0027 21 FC=(FC+FIF)*C.01745
0028 162 CONTINUE
0029 DO 776 I=1,L
0030 DO 776 J=1,20
0031 IF(B(I,J).EQ.90.) GO TO 414
0032 X(1)=-CCS(A(I,J))*SIN(B(I,J))
0033 X(2)=SIN(B(I,J))*SIN(A(I,J))
0034 X(3)=CCS(B(I,J))
0035 T1=(X(1)*SIN(F)+X(3)*CCS(F))*CCS(FC)
0036 T2=(-X(1)*COS(F)+X(3)*SIN(F))*SIN(FC)
0037 S(I,J)=C.0
0038 5 QC=CCS(FC)*CCS(F)*CCS(W)+SIN(FO)*SIN(F)
0039 Q1=1.0/(QD+0.0001)
0040 IF(Q1-2.8) 121, 121, 122
0041 122 IF(Q1.GE.2.9) Q1=2.9C
0042 IF(Q1.EE.3.0) C1=3.05
0043 IF(Q1.EE.3.1) C1=3.21
0044 IF(Q1.EE.3.3) C1=3.35
0045 IF(Q1.EE.3.5) C1=3.55
0046 IF(Q1.EE.3.7) C1=3.82
0047 IF(Q1.EE.4.0) C1=4.07
0048 IF(Q1.EE.4.6) C1=4.72
0049 IF(Q1.EE.5.0) C1=5.12
0050 IF(Q1.EE.5.5) C1=5.60
0051 IF(Q1.EE.6.0) C1=6.18
0052 IF(Q1.EE. 6.5) C1=6.88
0053 IF(Q1.EE. 8.0) C1=7.77
0054 IF(Q1.EE. 8.8) C1=8.50
0055 IF(Q1.EE.10.0) C1=10.35
0056 IF(Q1.EE.13.0) C1=12.44
0057 IF(Q1.EE.17.0) C1=15.36
0058 IF(Q1.EE.24.0) C1=19.75
0059 121 IF(ABS(C1).GT.45.0) C1=30.0
0060 Q2=-X(2)*SIN(W)*CCS(FO)+T1*CCS(W)
0061 CT=Q2+T2
0062 IF(CT.LT.C.C.CP.CT.LT.C.C) OT=C.0
0063 S(I,J)=S(I,J)+60.0*SCL*G**C1*OT
0064 S(I,J)=S(I,J)+DIF*(CCS(B(I,J)/2.0))**2
0065 GO TO 776
0066 414 S(I,J)=0.0
0067 776 CONTINUE
0068 WRITE (6,632) ((S(I,J), J=1,20), I=1,L)
0069 632 FCFMAT(2CF5,0)
0070 GO TO 661
0071 999 STOP
0072 END

```

Fig. 14 Computer Programme for Calculating Hourly
Global Radiation in Barbados

is then converted to radians in step 17.

The value of sky-diffuse radiation is supplied directly for the hour in question from the radiation observations of the site being used. To obtain the atmospheric transmissivity (G) it is necessary first to obtain the height of the sun above the horizon for the given hour. This is provided by a programme of which a print-out of results is illustrated in Fig. 15. In this example, the solar declination (ϕ_0) is for June 21st and shows that at 6 am solar time, hour angle (W) = 0.00, the height of the sun is 5.04° above the horizon in Barbados. The values for W are given every twenty minutes, from which the height of the sun at the mid-point of the relevant hour can be readily found. The results of a second programme (Fig. 16) are then used to obtain G by reference to the height of the sun above the horizon (EJ) and the value of the direct radiation, in langley's per minute (Q), observed at the station during the hour. These data are then inserted into the computer programme and the calculation of the global radiation at each grid-point of the base map proceeds in the usual way, with a digital print-out for results (Fig. 17).

It will have been noticed that neither in the mapping of hourly values nor of daily totals has any allowance been made for the influence of local sky-line obstruction on the topographic variation of radiation. A method to allow for this when necessary has been devised and incorporated into the computer calculations (Ohmura, 1969). However, analysis shows that the influence of a local sky-line is negligible on daily totals except in mountainous areas of middle and high latitudes, and for hourly values only when the sun is low and the local relief particularly rugged. It needs to be allowed for in the

FO	W	DEG	FO	W	DEG
0.40143	-1.57080	-53.99942	0.40143	1.57080	31.00018
0.40143	-1.48353	-53.66806	0.40143	1.65806	74.93057
0.40143	-1.39627	-52.69167	0.40143	1.74533	76.21150
0.40143	-1.30900	-51.11887	0.40143	1.83259	72.60124
0.40143	-1.22173	-49.01848	0.40143	1.91986	63.54701
0.40143	-1.13447	-45.46701	0.40143	2.00713	54.26014
0.40143	-1.04720	-43.53902	0.40143	2.09439	57.34225
0.40143	-0.95993	-40.30130	0.40143	2.18166	55.34641
0.40143	-0.87267	-36.81078	0.40143	2.26892	50.40255
0.40143	-0.78540	-33.11440	0.40143	2.35619	46.22905
0.40143	-0.69813	-29.25017	0.40143	2.44346	41.63812
0.40143	-0.61087	-25.24866	0.40143	2.53072	37.03824
0.40143	-0.52360	-21.13434	0.40143	2.61799	32.43599
0.40143	-0.43633	-16.92001	0.40143	2.70525	27.93672
0.40143	-0.34907	-12.64722	0.40143	2.79252	23.24507
0.40143	-0.26180	-8.29317	0.40143	2.87979	18.66544
0.40143	-0.17453	-3.89038	0.40143	2.96705	14.10216
0.40143	-0.08727	0.55739	0.40143	3.05432	9.55977
0.40143	0.00000	5.04275	0.40143	3.14158	5.04316
0.40143	0.08727	9.55939	0.40143	3.22885	0.55784
0.40143	0.17453	14.10182	0.40143	3.31612	-3.88990
0.40143	0.26180	18.66512	0.40143	3.40338	-8.29267
0.40143	0.34907	23.24478	0.40143	3.49065	-12.64169
0.40143	0.43633	27.83647	0.40143	3.57791	-16.92636
0.40143	0.52360	32.43578	0.40143	3.66518	-21.13377
0.40143	0.61087	37.03806	0.40143	3.75245	-25.24806
0.40143	0.69813	41.63797	0.40143	3.83971	-29.24956
0.40143	0.78540	46.22994	0.40143	3.92698	-33.11378
0.40143	0.87267	50.80246	0.40143	4.01424	-36.81018
0.40143	0.95993	55.34637	0.40143	4.10151	-40.30070
0.40143	1.04720	59.84221	0.40143	4.18878	-43.53844
0.40143	1.13447	64.26007	0.40143	4.27604	-46.46646
0.40143	1.22173	68.54701	0.40143	4.36331	-49.01801
0.40143	1.30900	72.60124	0.40143	4.45057	-51.11848
0.40143	1.39626	76.21146	0.40143	4.53784	-52.69138
0.40143	1.48353	79.93057	0.40143	4.62510	-53.66792
			0.40143	4.71237	-53.99942

Fig. 15 The Elevation of the Sun at Different Times on June 21 in Barbados

EJ	Q	G
29.00000	0.20000	0.65666
25.00000	0.20000	0.54383
30.00000	0.20000	0.44721
35.00000	0.20000	0.36719
40.00000	0.20000	0.30240
45.00000	0.20000	0.25080
50.00000	0.20000	0.21019
55.00000	0.20000	0.17857
60.00000	0.20000	0.15420
65.00000	0.20000	0.13565
70.00000	0.20000	0.12181
75.00000	0.20000	0.11185
80.00000	0.20000	0.10513
20.00000	0.30000	0.75434
25.00000	0.30000	0.64548
30.00000	0.30000	0.54772
35.00000	0.30000	0.46333
40.00000	0.30000	0.39244
45.00000	0.30000	0.33407
50.00000	0.30000	0.28676
55.00000	0.30000	0.24892
60.00000	0.30000	0.21907
65.00000	0.30000	0.19589
70.00000	0.30000	0.17830
75.00000	0.30000	0.16547
80.00000	0.30000	0.15673
20.00000	0.40000	0.83234
25.00000	0.40000	0.72893
30.00000	0.40000	0.63245
35.00000	0.40000	0.54645
40.00000	0.40000	0.47215
45.00000	0.40000	0.40943
50.00000	0.40000	0.35746
55.00000	0.40000	0.31507
60.00000	0.40000	0.28104
65.00000	0.40000	0.25424
70.00000	0.40000	0.23365
75.00000	0.40000	0.21847
80.00000	0.40000	0.20806
20.00000	0.50000	0.89835
25.00000	0.50000	0.80101
30.00000	0.50000	0.70711
35.00000	0.50000	0.62107
40.00000	0.50000	0.54497
45.00000	0.50000	0.47941
50.00000	0.50000	0.42409
55.00000	0.50000	0.37826
60.00000	0.50000	0.34096
65.00000	0.50000	0.31122
70.00000	0.50000	0.28816
75.00000	0.50000	0.27102
80.00000	0.50000	0.25920

Fig. 16 Atmospheric Transmissivity, Solar Radiation,
and Sun Angle, Barbados

DATE#19641215 DECLINATION#-23.13

TRANSMISSIVITY# C.708

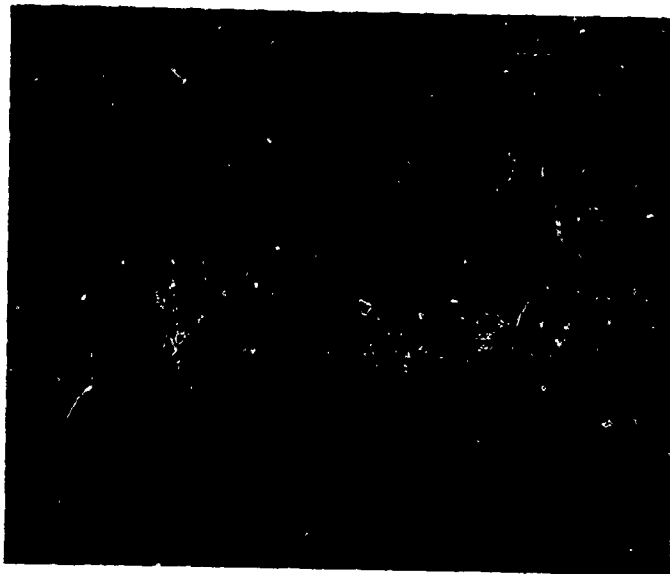
SKY-DIFFUSE INSOLATION# 8.0

TIME#-52.00

36.	33.	40.	31.	35.	36.	36.	35.	36.	35.	37.	35.	36.	0.	0.	0.	0.	0.	0.
35.	33.	21.	27.	34.	26.	29.	37.	35.	35.	35.	35.	35.	0.	0.	0.	0.	0.	0.
31.	34.	26.	37.	21.	35.	42.	36.	34.	35.	35.	35.	35.	0.	0.	0.	0.	0.	0.
35.	36.	30.	34.	35.	37.	41.	40.	30.	32.	26.	36.	35.	25.	0.	0.	0.	0.	0.
37.	34.	16.	36.	35.	36.	35.	36.	38.	34.	36.	35.	36.	24.	0.	0.	0.	0.	0.
35.	31.	31.	35.	35.	35.	35.	36.	40.	42.	33.	31.	39.	40.	0.	0.	0.	0.	0.
35.	29.	24.	36.	35.	35.	35.	35.	33.	40.	31.	31.	38.	34.	34.	0.	0.	0.	0.
35.	31.	36.	31.	25.	35.	35.	35.	35.	36.	39.	31.	39.	35.	27.	38.	0.	0.	0.
35.	35.	35.	35.	21.	21.	34.	33.	33.	36.	33.	31.	32.	33.	38.	51.	0.	0.	0.
0.	0.	0.	0.	35.	37.	29.	33.	34.	31.	34.	34.	32.	33.	49.	38.	39.	0.	0.
0.	0.	0.	0.	35.	32.	41.	34.	35.	33.	26.	30.	35.	35.	29.	42.	41.	0.	0.
0.	0.	0.	0.	0.	0.	0.	0.	34.	34.	33.	36.	43.	40.	43.	33.	44.	45.	0.
0.	0.	0.	0.	0.	0.	0.	0.	35.	35.	31.	31.	42.	39.	43.	31.	46.	38.	0.
0.	0.	0.	0.	0.	0.	0.	0.	34.	36.	26.	34.	39.	40.	36.	31.	45.	39.	0.
0.	0.	0.	0.	0.	0.	0.	0.	31.	30.	35.	35.	42.	37.	49.	45.	46.	35.	0.
0.	0.	0.	0.	0.	0.	0.	0.	33.	26.	31.	52.	44.	42.	49.	46.	41.	36.	0.
0.	0.	0.	0.	0.	0.	0.	0.	30.	31.	51.	45.	43.	39.	44.	44.	39.	37.	35.
0.	0.	0.	0.	0.	0.	0.	0.	32.	38.	43.	48.	45.	42.	41.	46.	39.	42.	39.
0.	0.	0.	0.	0.	0.	0.	0.	34.	45.	47.	48.	39.	41.	39.	41.	39.	39.	37.
0.	0.	0.	0.	0.	0.	0.	0.	41.	45.	45.	45.	45.	41.	37.	40.	26.	44.	35.
0.	0.	36.	34.	27.	31.	44.	34.	37.	49.	42.	44.	44.	37.	42.	48.	39.	35.	33.
0.	0.	31.	35.	34.	34.	44.	44.	40.	46.	40.	44.	41.	41.	45.	40.	35.	35.	32.
0.	0.	29.	34.	31.	42.	41.	41.	41.	45.	34.	41.	40.	40.	36.	35.	35.	29.	35.
0.	0.	33.	33.	31.	42.	37.	43.	44.	46.	44.	41.	39.	37.	37.	24.	27.	43.	24.
0.	0.	33.	34.	31.	42.	49.	45.	37.	41.	37.	37.	35.	30.	26.	19.	35.	28.	34.
0.	0.	32.	31.	34.	52.	37.	41.	37.	32.	39.	37.	32.	30.	46.	41.	38.	40.	35.
0.	0.	39.	32.	34.	46.	34.	34.	40.	48.	40.	34.	31.	26.	42.	41.	39.	37.	39.
0.	0.	23.	35.	36.	46.	45.	48.	47.	51.	42.	39.	21.	35.	44.	32.	31.	31.	35.
0.	0.	31.	31.	49.	35.	44.	42.	51.	40.	37.	37.	45.	41.	38.	35.	31.	44.	36.
0.	0.	35.	35.	43.	45.	43.	46.	27.	44.	46.	41.	34.	36.	35.	31.	21.	30.	45.
0.	0.	31.	35.	42.	48.	38.	38.	34.	36.	28.	30.	35.	47.	20.	24.	15.	50.	48.
0.	0.	33.	33.	35.	36.	48.	35.	39.	26.	27.	46.	29.	35.	22.	49.	43.	42.	39.
0.	0.	31.	30.	50.	41.	45.	45.	36.	27.	41.	44.	21.	33.	21.	40.	30.	42.	30.
0.	0.	33.	27.	43.	49.	42.	30.	33.	42.	42.	33.	21.	25.	24.	28.	36.	34.	28.
0.	0.	32.	27.	37.	30.	33.	40.	38.	33.	39.	30.	21.	25.	35.	48.	51.	19.	52.
0.	0.	31.	26.	31.	46.	51.	35.	34.	31.	36.	32.	21.	24.	22.	44.	26.	28.	54.
0.	0.	34.	28.	45.	43.	40.	27.	31.	31.	36.	42.	17.	20.	48.	48.	42.	48.	46.
0.	0.	0.	0.	0.	29.	46.	29.	30.	32.	40.	43.	30.	11.	51.	19.	7.	54.	51.
0.	0.	0.	0.	0.	21.	32.	34.	31.	30.	35.	37.	21.	49.	28.	26.	26.	43.	35.
0.	0.	0.	0.	0.	24.	28.	23.	30.	30.	26.	24.	50.	22.	23.	51.	44.	45.	30.
0.	0.	0.	0.	0.	34.	35.	35.	21.	25.	37.	36.	50.	19.	27.	40.	49.	40.	36.
0.	0.	0.	0.	0.	35.	31.	33.	30.	36.	44.	51.	28.	23.	24.	52.	40.	39.	34.
0.	0.	0.	0.	0.	21.	35.	29.	35.	24.	25.	19.	40.	44.	42.	37.	36.	31.	26.
0.	0.	0.	0.	0.	36.	30.	26.	41.	39.	32.	43.	26.	46.	46.	41.	41.	26.	31.
0.	0.	0.	0.	0.	21.	25.	40.	40.	33.	22.	37.	25.	57.	48.	43.	30.	20.	31.
0.	0.	0.	0.	0.	39.	33.	31.	21.	44.	32.	29.	41.	51.	44.	40.	29.	27.	36.
0.	0.	0.	0.	0.	31.	31.	33.	40.	31.	34.	35.	42.	42.	40.	27.	23.	30.	21.
0.	0.	0.	0.	0.	35.	33.	30.	34.	34.	34.	27.	45.	45.	30.	26.	23.	35.	21.
0.	0.	0.	0.	0.	34.	30.	31.	21.	27.	28.	28.	44.	50.	28.	23.	35.	16.	23.
0.	0.	0.	0.	0.	35.	31.	35.	27.	27.	40.	29.	34.	26.	38.	30.	27.	26.	27.
0.	0.	0.	0.	0.	32.	34.	20.	39.	29.	35.	34.	40.	31.	30.	26.	27.	36.	21.
0.	0.	0.	0.	0.	33.	25.	29.	21.	27.	34.	34.	35.	29.	39.	38.	36.	30.	35.
0.	0.	0.	0.	0.	22.	34.	32.	35.	31.	31.	40.	38.	39.	36.	37.	37.	35.	25.

Fig. 17 A Sample of Hourly Radiation Values,
Barbados

tropics, therefore, only under exceptional circumstances, when for example, a detailed study over short time periods is underway. In Barbados, the local relief is nowhere so strong as to influence materially the distribution pattern of global radiation at the scale of the present study. Consequently, no allowance has been made for such an influence in the work discussed in this report.



Radiation equipment at Brace Experimental Station. Upper photo: Kipp solarimeter. Lower photo: shielded silicon cell, with Campbell-Stokes sunshine recorder nearby.

IV

SELECTED GLOBAL RADIATION MAPS OF BARBADOS

The methods of calculation and the computer programming which have been described have been used to make a number of global radiation maps of Barbados. These are somewhat preliminary in nature, and it is not the purpose of this report to offer either a detailed analysis of them or a substantive scientific interpretation of the results which they show. Some general comments on a few of the maps, however, may serve to illustrate further the scope and usefulness of the procedures which have been developed.

All the data for the maps illustrated here were derived from observations made in 1964 at the Brace Experiment Station, located in the grounds of the Bellairs Research Institute on the west coast of the island (Tout, 1968). An Eppley pyranometer and a Kipp and Zonen pyranometer, both calibrated at the Canadian Meteorological Headquarters in Toronto, were used interchangeably for measuring global radiation. A silicon cell unit, with a shadow band, was used for the sky-diffuse component. Corrections were made to allow for the fraction of the radiation screened by the shadow band itself, and the resulting values were subtracted from measured global radiation values to obtain the value of direct solar radiation.

The instruments were connected to Honeywell strip chart recording potentiometers, the continuous record thus obtained being analysed by hand to obtain hourly values. There was some obstruction

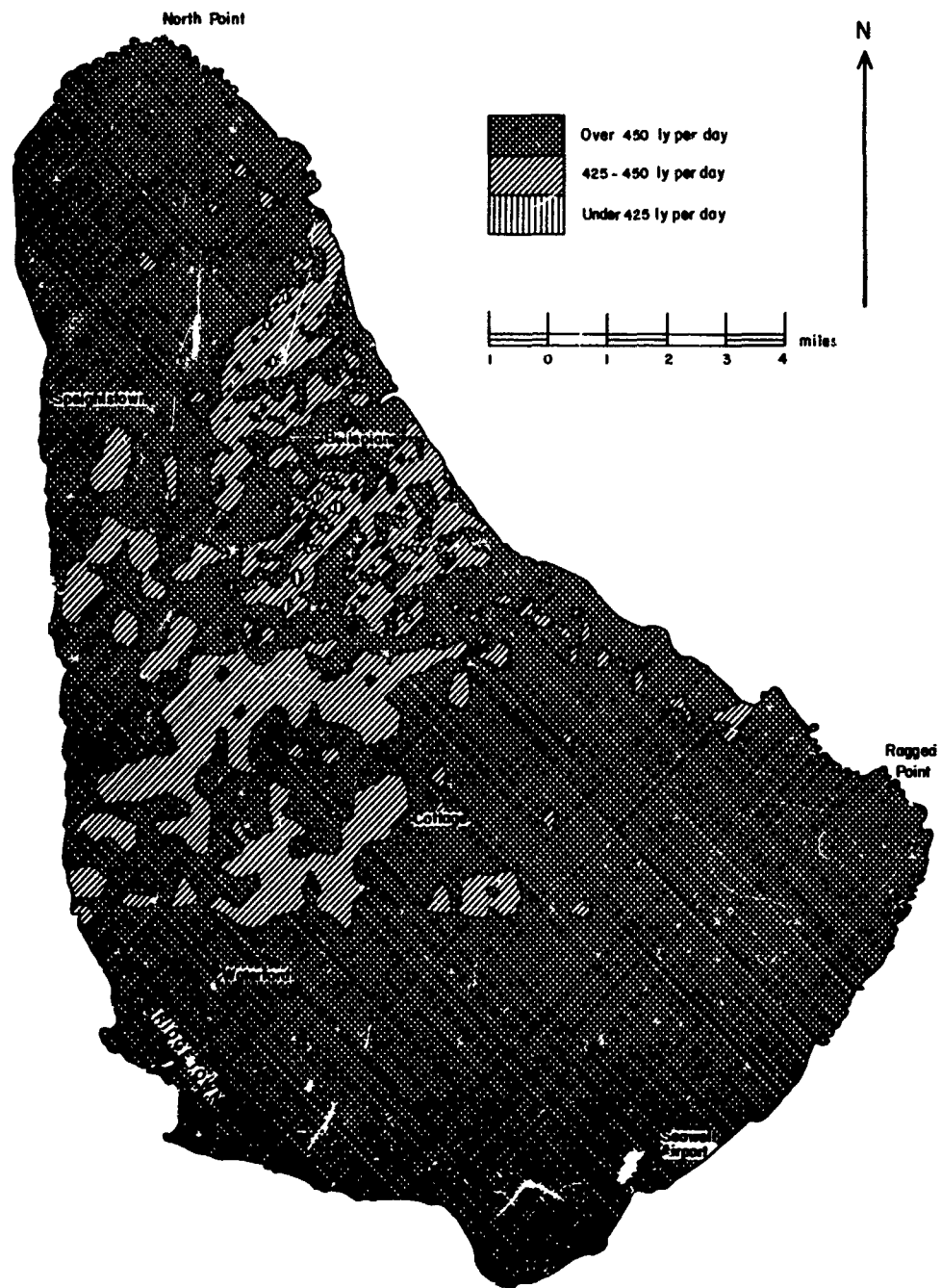


Fig. 18 Mean Daily Distribution of Global Radiation
in Barbados, July, 1964

to the site by trees. This influenced daily totals by no more than a maximum of 3% (Tout, 1967). However, the presence of the obstruction means that the records near the beginning and end of each day are unreliable for hourly analyses.

TABLE THREE
Mean Daily Radiation Totals for Selected Months, 1964
(langleys per day)

Month	Direct	Sky-Diffuse	Global
July	241	210	451
September	212	199	411
December	318	114	432

The first three maps used as illustration (Figs. 18, 19, 20), show the mean daily value of surface variation in global radiation for July, September, and December, 1964. It is interesting to note from Table Three that the mean daily value of global radiation recorded for each of these months was rather similar. This similarity from one month to another is a feature of global radiation observations in the tropics when such measurements are confined to instruments well-exposed in a horizontal position. Figs. 18, 19, and 20, however, show that such similarity successfully hides the topographic variation which actually exists. This variation is expressed in the maps illustrated partly by the range of values over the island, and partly by the actual spatial pattern. The former are low, approximately 30 langleys per day, in the two high sun months of July and September, but the range exceeds 100

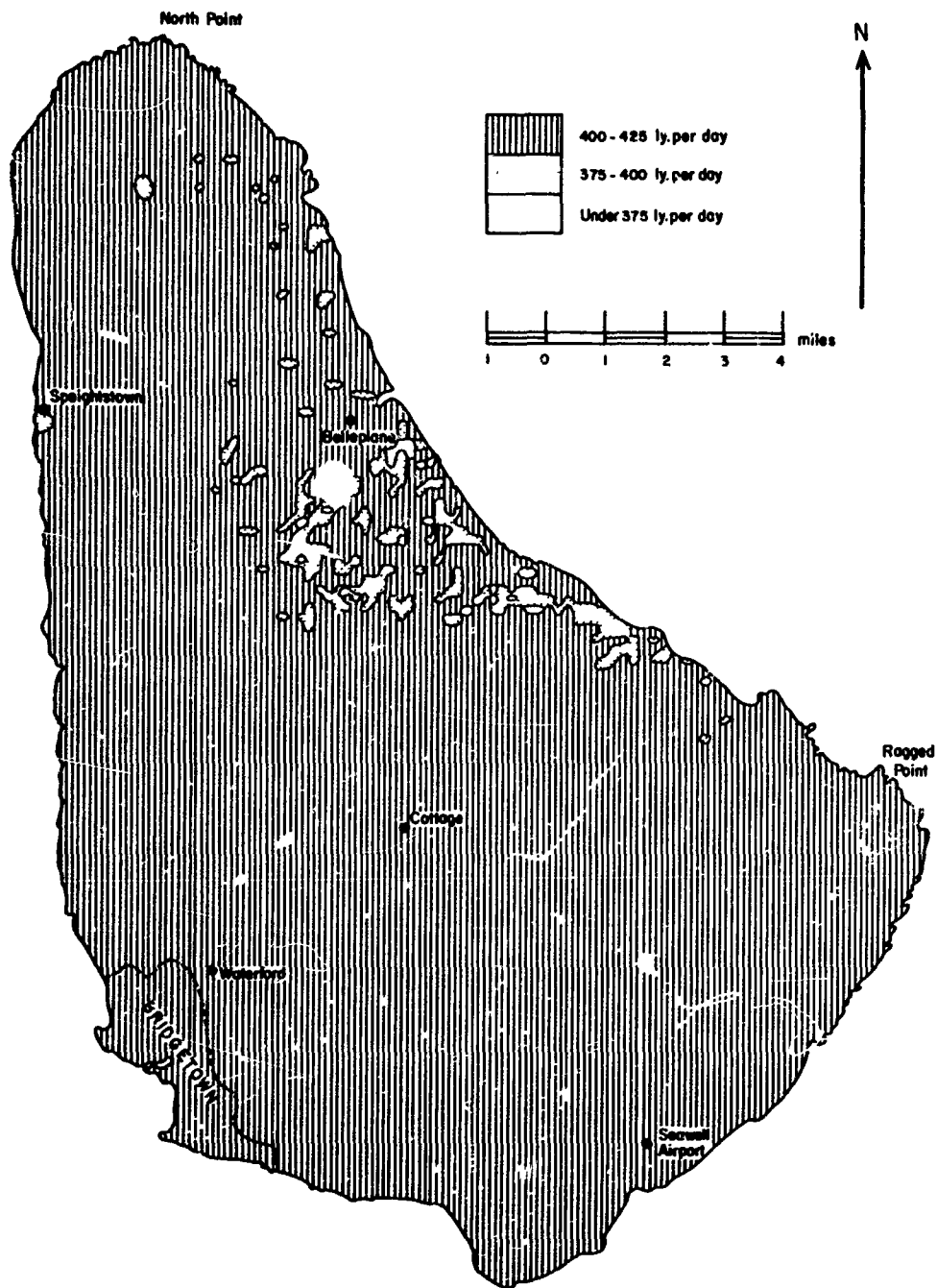


**Fig. 19 Mean Daily Distribution of Global Radiation
in Barbados, September, 1964**

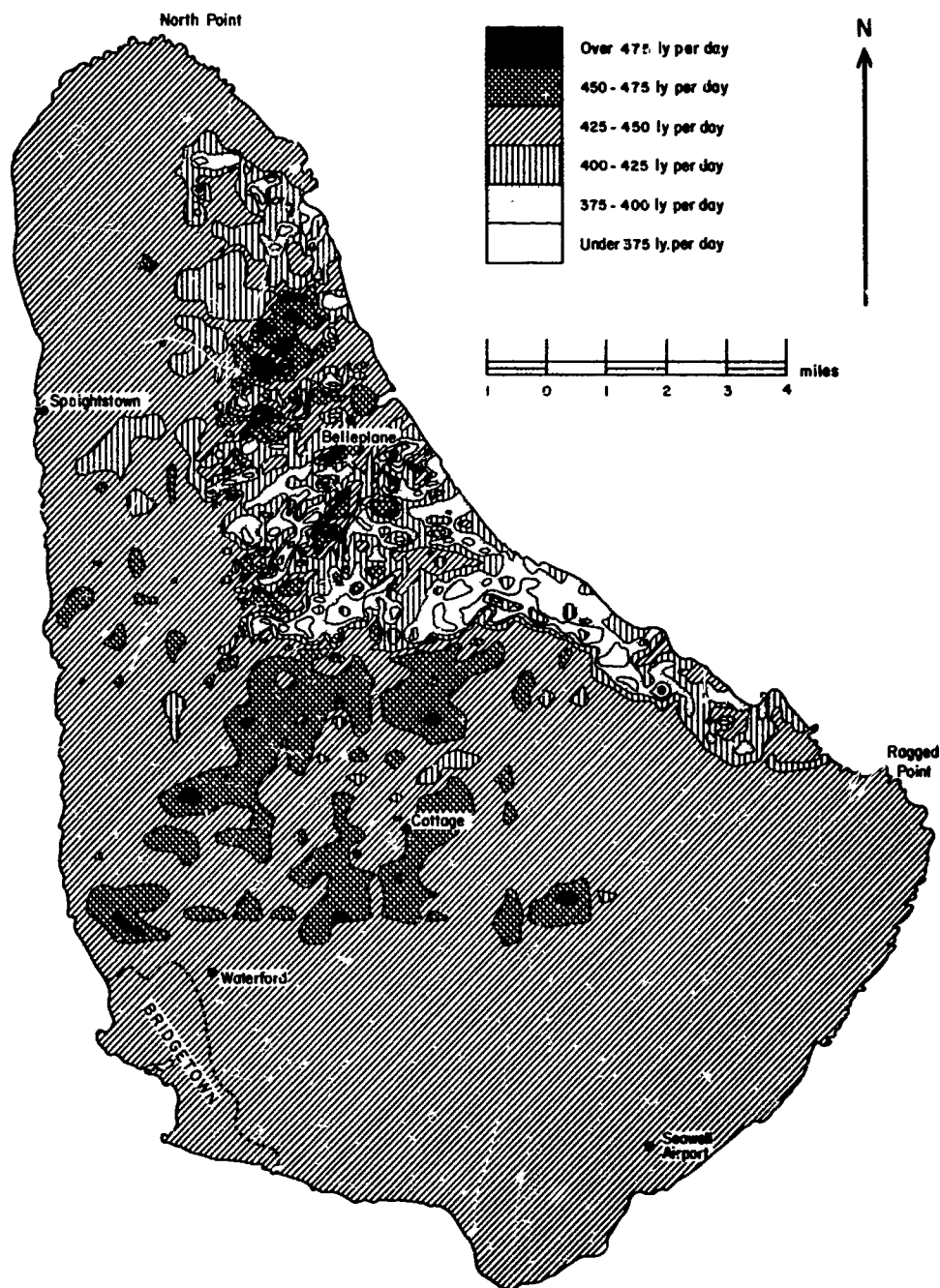


Fig. 20 Mean Daily Distribution of Global Radiation in Barbados, December, 1964

langleys per day in December. There is, however, more spatial variety in the July map than in the September map. This may be explained by the fact that the sun is further from the zenith at noon over Barbados in July than in September, especially during the early part of the month. The relatively low range, however, reflects the comparatively large contribution of sky-diffuse radiation to global radiation totals (Table Three) since sky-diffuse radiation is not as sensitive as direct solar radiation to topographic influence.

In December, 1964, some 75% of the global radiation total was direct. With the sun at its lowest elevation of the year during this month, the resulting spatial pattern expressed considerable diversity. The influence of surface geometry on the spatial distribution of the direct radiation component under these conditions is accordingly manifested in the large range of daily values from place to place during this month.

A specific example of the influence of solar elevation, even in the tropics, when the direct component in global radiation totals is high, is illustrated in Figs. 21 and 22. The measured direct radiation totals on the two days shown were almost identical: 438 langleys on June 18, and 436 langleys on December 28. Sky-diffuse radiation for the two dates was 152 langleys and 74 langleys respectively. The resulting totals of global radiation, 590 langleys for June 18 and 510 langleys for December 28, are typical of the general range of radiation values in the tropics when measurements are confined to the horizontal. A much greater contrast is apparent when the element of topographic variation is introduced.

In comparing Fig. 21 with Fig. 22 it must be noted that the

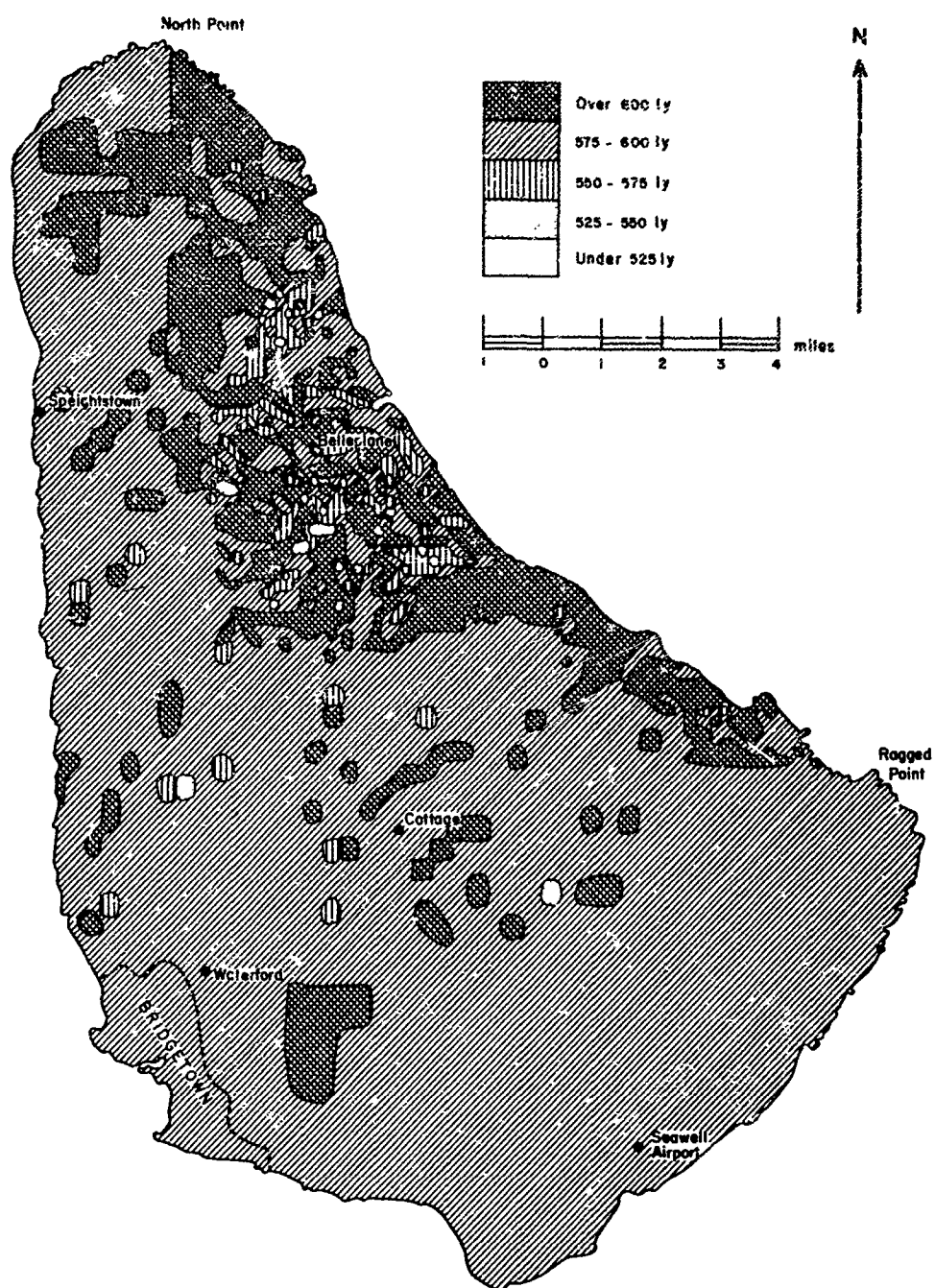
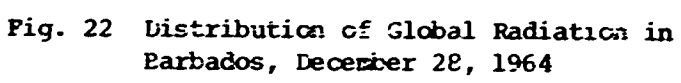


Fig. 21 Distribution of Global Radiation in:
Barbados, June 18, 1964



scale of shading differs from one map to the other. The June map has an isarithmic interval of 25 langleys and that for December of 75 langleys. The cartographic problem of showing adequately the two patterns by the same isarithmic interval at the scale permissible at the page size of this report, itself underlines the contrast between the surface variations of global radiation on the two dates. The range of values on June 18 was little more than 75 langleys; that for December 28 exceeded 225 langleys. Thus, an interval of 75 langleys for the June map would have suggested a topographic uniformity which did not, in fact, exist, while a 25- langley interval for the December map would have produced a complexity too great to be shown on a small-scale map. These comments alone emphasize the contrasts in the topographic variation of global radiation during the two days -- two days with generally similar solar radiation totals, and an atmospheric transmissivity and pattern of cloud characteristic of a clear Barbados day.

The remaining maps illustrate mapping on the basis of hourly radiation values. An example for a specific date, June 18, 1964, is given in Figs. 23 and 24. The morning hour chosen, 0800-0900 hours, is the first hour of the day in which the observing instruments were clearly unaffected by the obstructions referred to earlier as existing at the site. The midday hour was chosen for comparison because the sun was then at its highest elevation of the day.

The day in question was clear to begin with, but clouds developed later. Thus of the 47 langleys recorded on a horizontal surface between 0800 and 0900 hours, 38 were contributed by direct radiation. By contrast, one-third of the 70 langleys recorded between 1200 and 1300 hours were contributed by sky-diffuse radiation. Whereas atmospheric transmissivity

was 0.80 in the morning hour it had been reduced to 0.63 by midday.

Comparison of the two maps shows clearly the greater spatial diversity at the morning hour and also the higher radiation income of the east-facing slopes than at midday. Indeed, some areas, such as northwest of Belleplane, changed little in the value of their global radiation income between the morning hour and midday, whereas the rest of the island experienced an increased radiation total as the sun approached its highest point.

The monthly maps of mean values in December (Figs. 25 and 26) also shows a tendency for east-facing slopes to have a relatively high global radiation income in the morning hour. That is not true, however, of the two July maps (Figs. 27 and 28). The difference may be related to the contrasts in the contribution of direct radiation to global hourly totals in the two months (Table Four). Whereas in December the mean daily contribution of direct radiation was 76% at 0800-0900 hours and 73% at 1200-1300 hours, in July the contributions at the same hours were both 57%.

TABLE FOUR

SELECTED MEAN HOURLY RADIATION TOTALS, 1964

Month	Time	Direct	Sky-Diffuse	Global
July	0800-0900	20	15	35
	1200-1300	34	26	60
December	0800-0900	26	8	34
	1200-1300	44	16	60

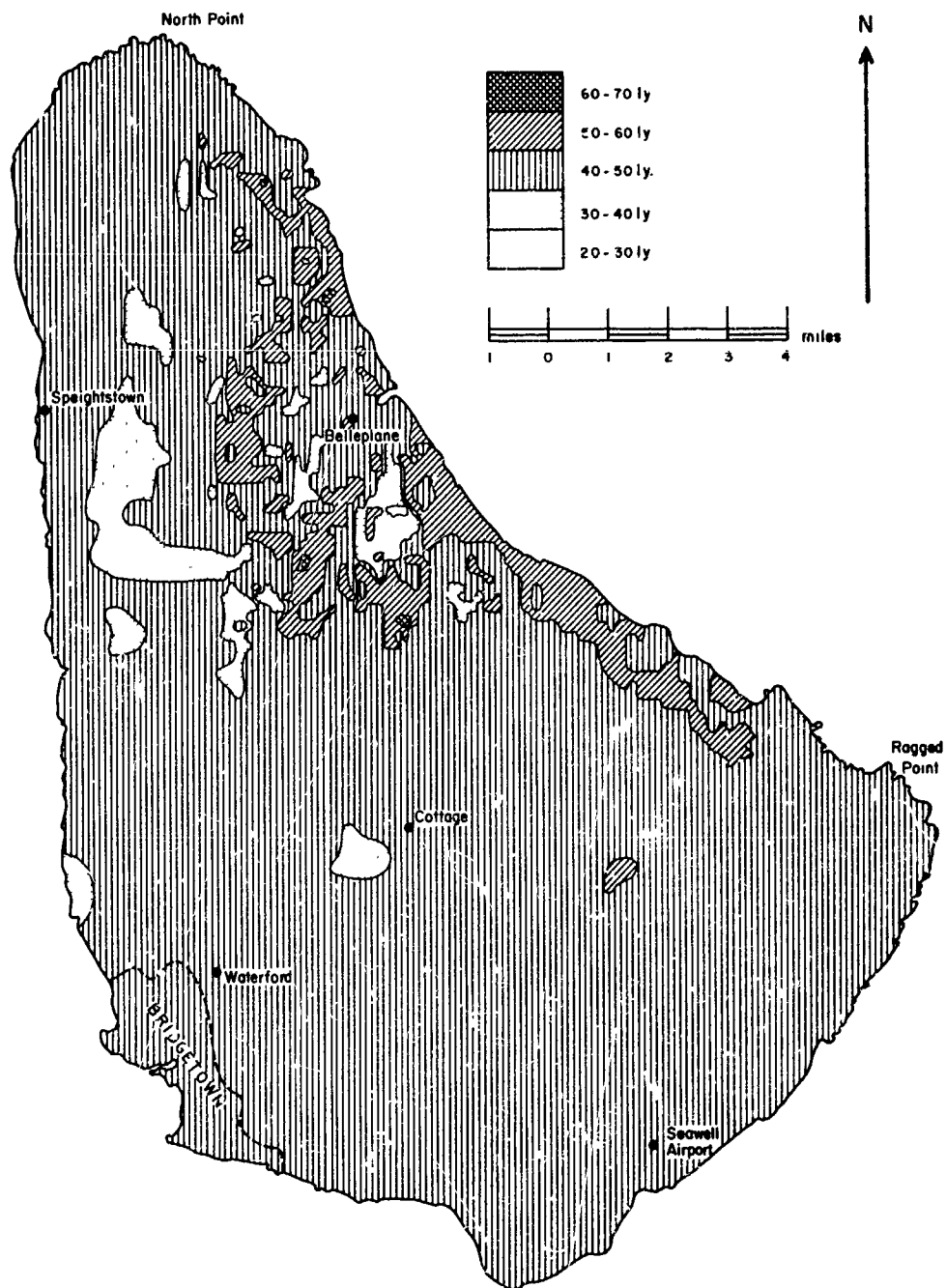


Fig. 23 Distribution of Global Radiation in
Barbados, 0800-0900 hours, June 18, 1964

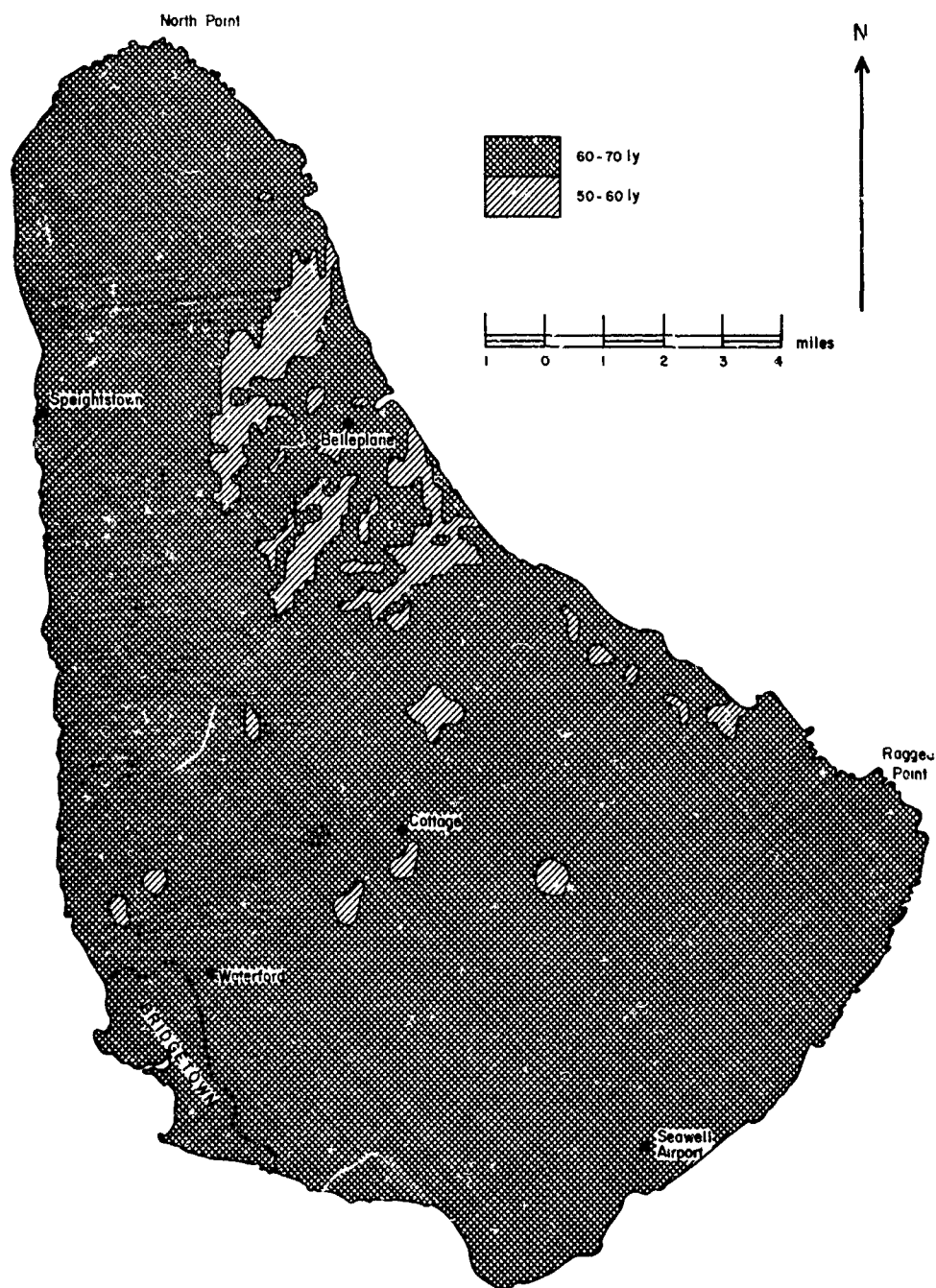


Fig. 24 Distribution of Global Radiation in Barbados,
1200 - 1300 hours, June 18, 1964

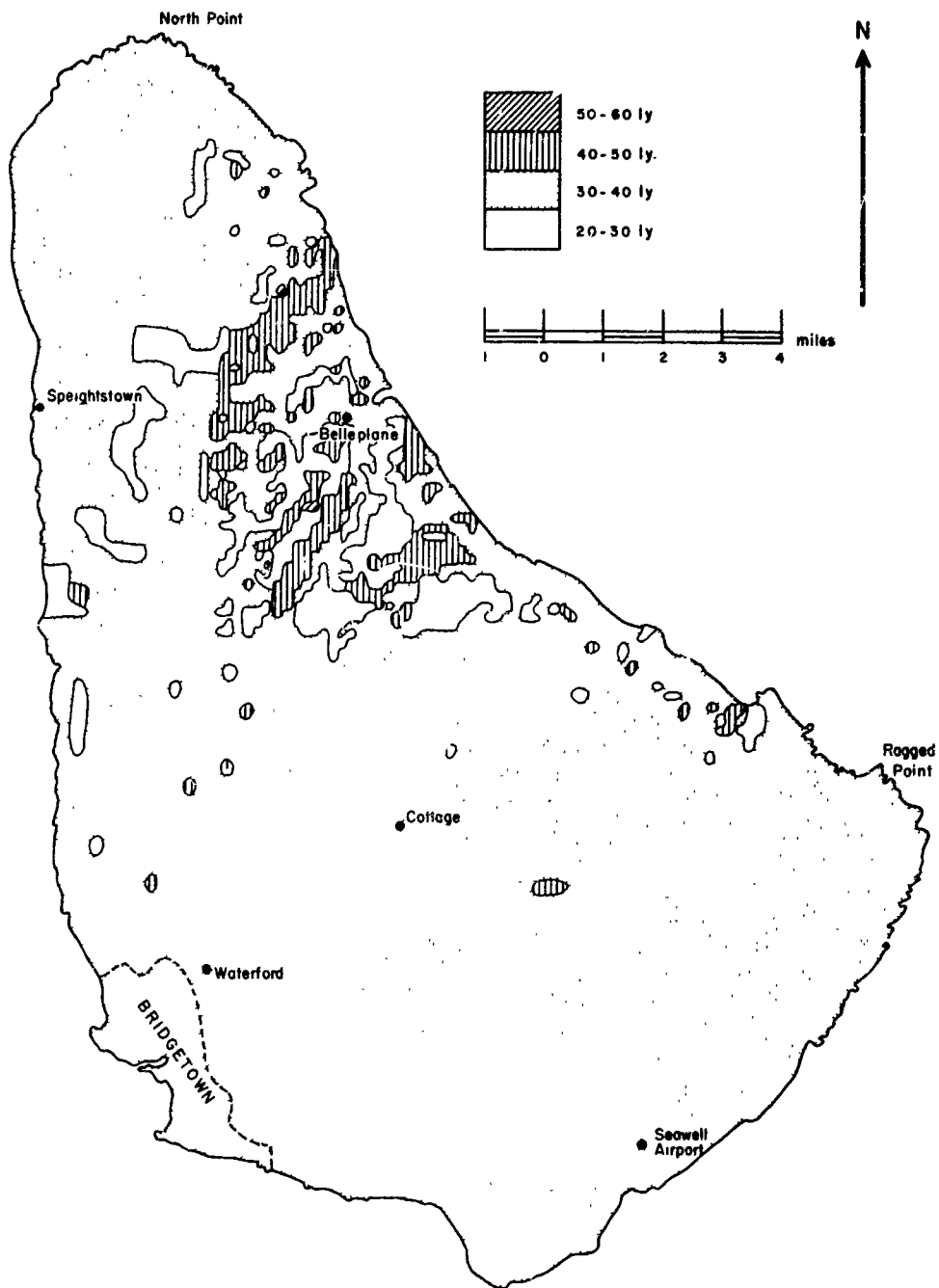


Fig. 25 Mean Value of Global Radiation, Barbados
0800-0900 hours, December 1964

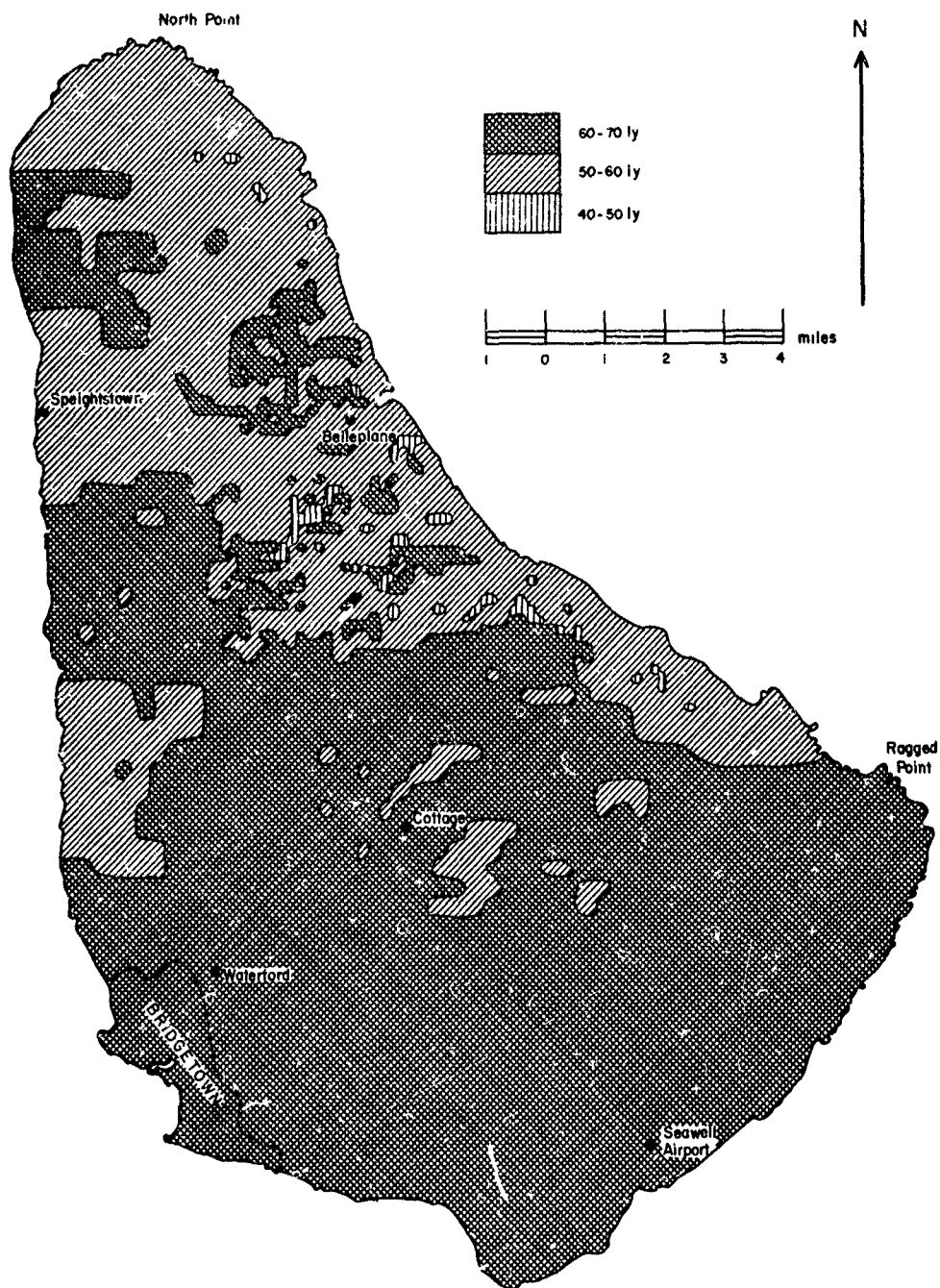


Fig. 26 Mean Value of Global Radiation, Barbados,
1200-1300 hours, December 1964

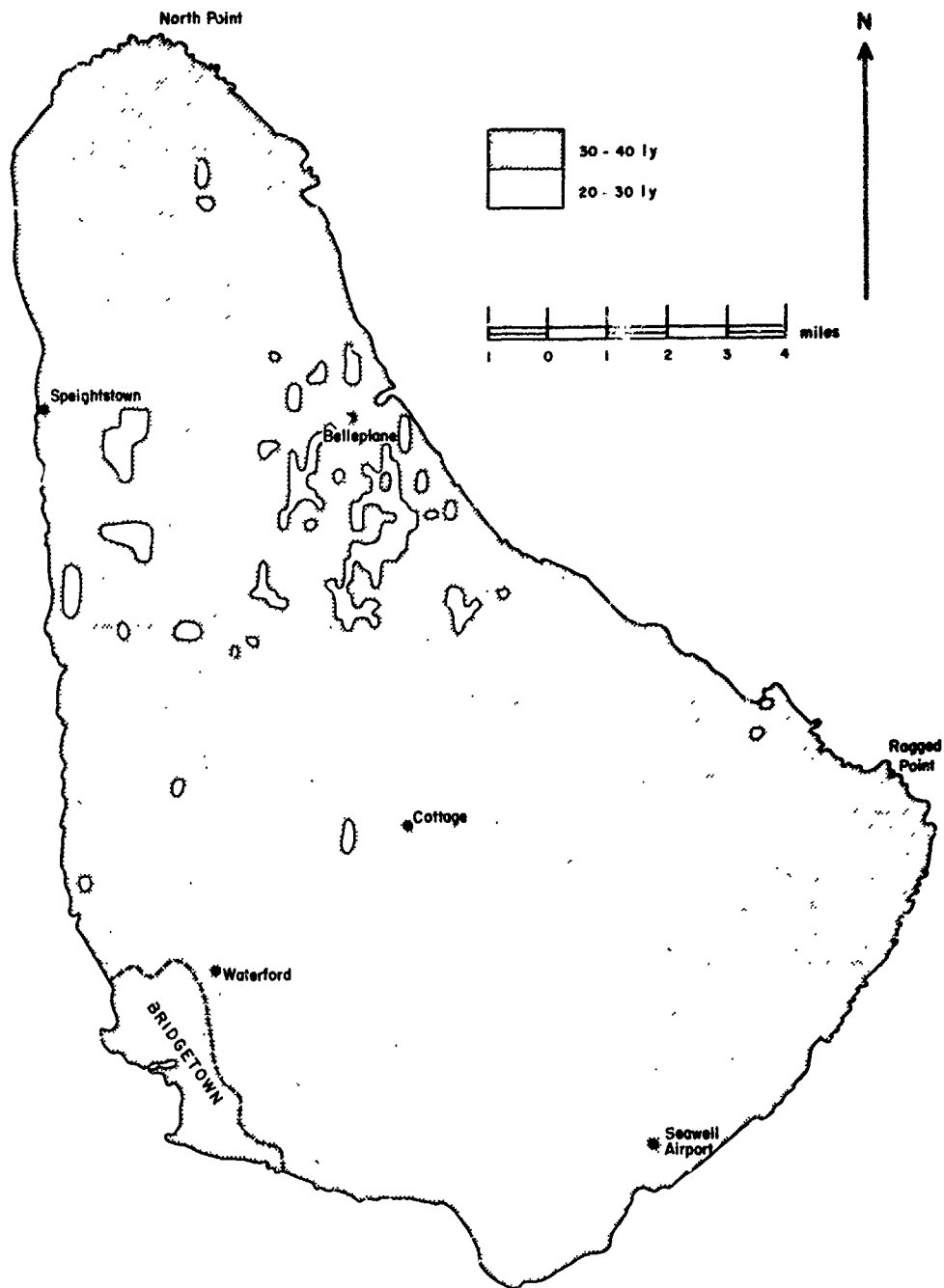


Fig. 27 Mean Value of Global Radiation Barbados,
0800-0900 hours, July, 1964

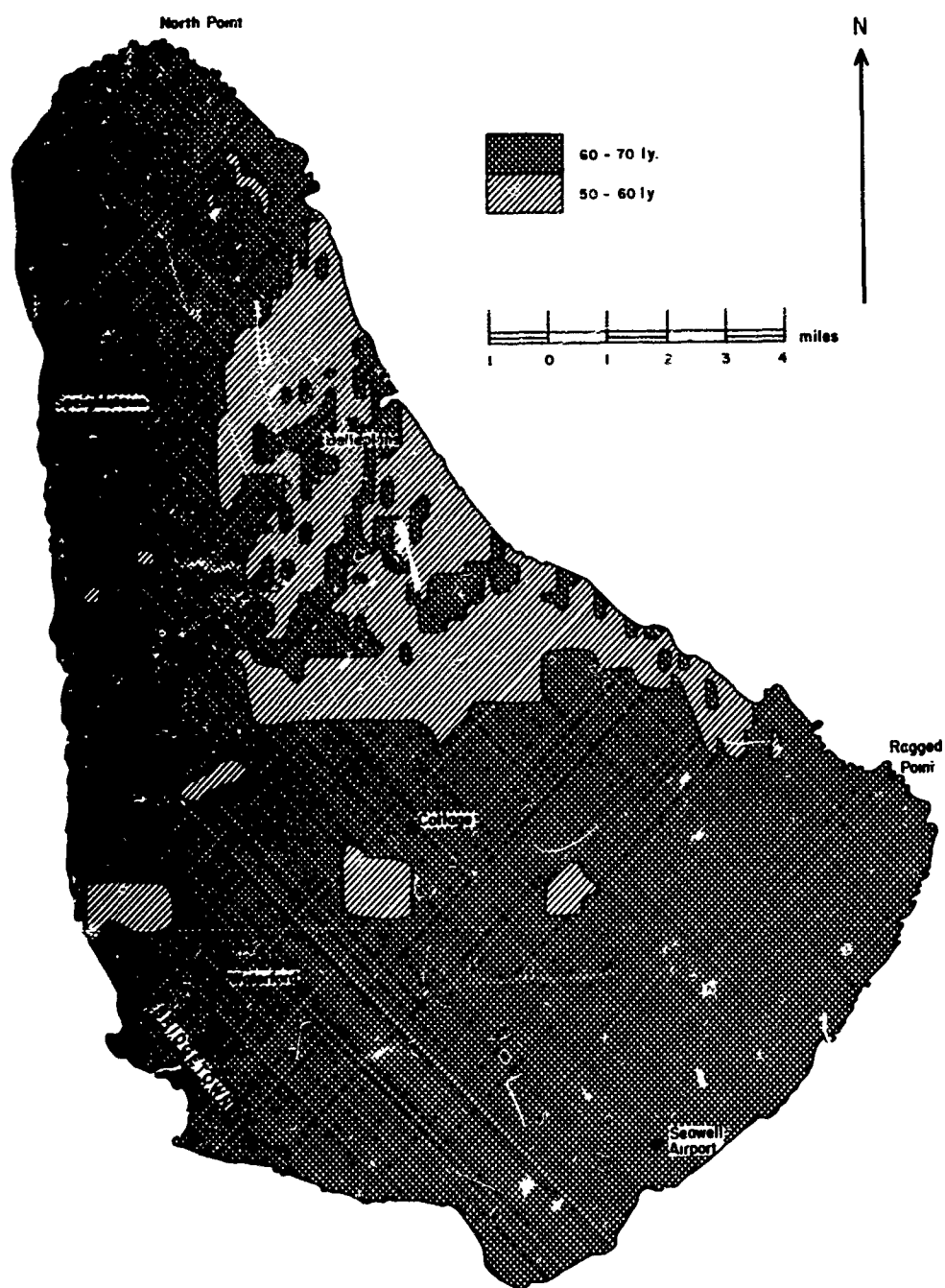


Fig. 28 Mean Value of Global Radiation, Barbados,
1200-1300 hours, July, 1964

V

CONCLUSION

The aim of this report has been to outline and explain methods which have been developed to portray the topographic variations in global radiation by using the radiation observations of a single, representative site. The sample maps used as illustration provide an indication of what the method reveals in a tropical context. Brief and superficial as are the comments made on the latter, it would appear that the principal conclusion which can be drawn is that, even in the tropics and in an area of generally only moderate relief, the actual surface variation of global radiation totals and intensities are greater than the normally made observations imply. These variations not only provide an important surface pattern at a given time, but also vary in their character at different times of year and under different weather conditions. In an atmosphere as sensitive to disturbance as the humid atmosphere of the Barbados region, small variations in the surface radiation may well have important consequences for convective development through the day. For this reason alone a fuller investigation of the pattern of short-wave radiation income revealed by the preliminary maps of this report seems worthwhile.

There are, however, wider implications. Many aspects of economic development are related to a knowledge of surface radiation balance. This is particularly so in relation to problems of agricultural development, plant growth, and water supply. To understand better the topographic variations of the surface energy budget is a first step towards a better

understanding of the ecological environment. The diversity of this environment is intimately related to the diversity revealed by this application of the analytical and mapping methods outlined in this report. Tropical environments are, indeed, not nearly so uniform as one is often led to suppose.

REFERENCES

- Basnayake, B.K., 1968: "Two Maps of Direct Shortwave Radiation in Barbados"
Climatol. Bulln. (McGill Univ.), No. 4, pp. 21-30.
- Brichambault, Perrin de, 1963: Rayonnement Solaire et Echanges Radiatifs Naturels, Gauthier-Villars, Paris.
- Garnier, B.J., 1968: "Estimating the Topographic Variation of Direct Solar Radiation: a contribution to geographical microclimatology",
Can. Geogr., Vol. 12, pp. 241-248.
- Garnier, B.J. and Atsumu Ohmura, 1968: "A Method of Calculating the Direct Shortwave Radiation Income of Slopes", Journ. Appl. Meteor., Vol. 11, pp. 796-800.
- Garnier, B.J. and Atsumu Ohmura (in press): "The Evaluation of Surface Variations in Shortwave Radiation Income" to appear in Solar Energy.
- Garstang, Michael & N.E. LaSeur, 1968: "The 1968 Barbados Experiment",
Bulln. Am. Meteor. Soc., Vol. 49, pp. 627-635.
- Hadley, G., 1935: "Concerning the cause of the General Trade Winds",
Philosophical Trans., Vol. 39, p.58.
- Haltiner, G.J. and F.L. Martin, 1957: Dynamical and Physical Meteorology, McGraw Hill Book Co., New York & London.
- Kondrat'yev, K.Ya., 1965: Radiative Heat Exchange in the Atmosphere, Pergamon Press, London & New York (translated from the Russian by O. Tedder).
- Kuettner, Joachim P. and Joshua Holland, 1969: "The BOMEX Project",
Bulln. Am. Meteor. Soc., Vol. 50, pp. 394-403.
- List, R.J., 1966: Smithsonian Meteorological Tables, Smithsonian Misc. Coll., Vol. 114, 6th edn.
- Ohmura, Atsumu, 1968: "The Computation of Direct Insolation on a Slope",
Climatol. Bulln., (McGill Univ.), No. 3, pp. 42-53.
- Ohmura, Atsumu, 1969: "Computation and Mapping the Shortwave Radiation on a Slope", M.Sc. Thesis, McGill University, Montreal.
- Robinson, N. (ed), 1966: Solar Radiation, Elsevier Publishing Co., Amsterdam.
- Simpson, G.C., 1930: "The Distribution of Terrestrial Radiation",
Mem. Roy. Meteor. Soc., Vol. 3, pp. 53-78.

Tout, D.G., 1967: "An Analysis of the 1964 Solar Radiation Record at the Brace Experiment Station, St. James, Barbados", Climat. Bulln. (McGill Univ.) No. 2, pp. 29-44.

Tout, D.G., 1968: "Tables of Radiation in Barbados, 1964", Climat. Obs. (N.S.), No. 2, McGill Univ.

LIST A

LIST OF RECIPIENTS OF THE REPORT

Chief of Naval Research Attention Geography Branch Code 44 Office of Naval Research Washington, D.C. 20360	2 copies
Defense Documentation Center Cameron Station Alexandria, Virginia 22314	20 copies
Director, Naval Research Laboratory Attention Technical Information Officer Washington, D.C. 20390	6 copies
Contract Admin. Southeastern Area Office of Naval Research 2110 G. Street, N.W. Washington, D.C. 20037	
Commanding Officer Office of Naval Research Branch Office Box 39 Fleet Post Office New York, New York 09510	
Chief of Naval Research Ocean Science and Technology Group Code 408 Office of Naval Research Washington, D.C. 20360	
Defense Intelligence Agency DIAAP-1E5 Meteorology Department of Defense Washington, D.C. 20301	
Chief of Naval Operations OP 09 B7, Naval Weather Washington, D.C. 20350	
Headquarters, Air Weather service Scott Air Force Base Illinois 62225	

DOCUMENT CONTROL DATA - R & D

(Security classification of title, body of abstract and indexing annotation must be entered when the overall report is classified)

1. ORIGINATING ACTIVITY (Corporate author) McGill University		2a. REPORT SECURITY CLASSIFICATION UNCLASSIFIED	
		2b. GROUP	
3. REPORT TITLE Estimating the Topographic Variations of Short-Wave Radiation Income in tropical regions: the example of Barbados			
4. DESCRIPTIVE NOTES (Type of report and inclusive dates) Technical Report			
5. AUTHOR(S) (First name, middle initial, last name) Garnier, B.J. and Ohmura, Atsumu			
6. REPORT DATE October, 1969		7a. TOTAL NO. OF PAGES 70	7b. NO. OF REFS 17
8a. CONTRACT OR GRANT NO. N00014-68-C-0307		9a. ORIGINATOR'S REPORT NUMBER(S) Technical Report No.1	
b. PROJECT NO. NR 389-152			
c.		9b. OTHER REPORT NO(S) (Any other numbers that may be assigned this report)	
d.			
10. DISTRIBUTION STATEMENT This document has been approved for public release and sale; its distribution is unlimited.			
11. SUPPLEMENTARY NOTES		12. SPONSORING MILITARY ACTIVITY Geography Branch, Office of Naval Research, Washington D.C. 20360	
13. ABSTRACT The surface pattern of short wave radiation can be estimated from the observations of a single, representative site provided it is possible to distinguish between direct and sky-diffuse radiation totals. The patterns of direct radiation over an area can then be mapped from the observations normally taken on a horizontal surface, and a knowledge of (1) extra terrestrial radiation, (2) the latitude, and (3) the surface geometry of the given area. Sky-diffuse radiation can be mapped by reference to the observations normally taken and the angles of slope over the area. Application of these methods to Barbados with the aid of a computer mapping program shows how varied the seasonal patterns of short-wave radiation income can in fact be in a tropical region of moderately diverse relief, despite the general similarity of recordings on a horizontal surface. The method also brings out the importance of the first three hours of the day to the heating of east facing slopes.			

